



## Scholars' Mine

---

Masters Theses

Student Theses and Dissertations

---

Fall 2008

# Recovery of materials from recycling of spent furnace linings

Phani Krishna Angara Raghavendra

Follow this and additional works at: [https://scholarsmine.mst.edu/masters\\_theses](https://scholarsmine.mst.edu/masters_theses)

 Part of the [Materials Science and Engineering Commons](#)

Department:

---

### Recommended Citation

Angara Raghavendra, Phani Krishna, "Recovery of materials from recycling of spent furnace linings" (2008). *Masters Theses*. 4631.

[https://scholarsmine.mst.edu/masters\\_theses/4631](https://scholarsmine.mst.edu/masters_theses/4631)

This thesis is brought to you by Scholars' Mine, a service of the Missouri S&T Library and Learning Resources. This work is protected by U. S. Copyright Law. Unauthorized use including reproduction for redistribution requires the permission of the copyright holder. For more information, please contact [scholarsmine@mst.edu](mailto:scholarsmine@mst.edu).



RECOVERY OF MATERIALS FROM RECYCLING  
OF SPENT FURNACE LININGS

by

PHANI KRISHNA ANGARA RAGHAVENDRA

A THESIS

Presented to the Faculty of the Graduate School of the  
MISSOURI UNIVERSITY OF SCIENCE AND TECHNOLOGY

In Partial Fulfillment of the Requirements for the Degree

MASTER OF SCIENCE IN MATERIALS SCIENCE AND ENGINEERING

2008

Approved by

Kent D. Peaslee, Advisor

Von L. Richards

Jeffrey D. Smith

© 2008

Phani Krishna Angara Raghavendra

All Rights Reserved

## ABSTRACT

The objective of this research study is to evaluate the technical feasibility of liberating metal entrapped in the spent melting furnace linings obtained from a non-ferrous metal producer and develop an economic technique to recycle all of the materials presently landfilled. Five to six million pounds of spent melting furnace linings are landfilled annually from this non-ferrous producer.

Samples from different types of refractory linings were characterized by scanning electron microscopy (SEM) and energy dispersive spectroscopy (EDS) to determine the size, shape and form of the metallic content in the ceramic matrix and predict possible metal penetration mechanisms. Crushing and grinding were used to liberate brass through the formation of strips which could be separated from the crushed refractory by screening. In the laboratory trials, 70% to 90% of the brass was recovered in a high copper product (~90% Cu) which could be directly re-melted. A refractory mix was developed to recycle the remaining crushed refractory size fractions by mixing with virgin refractory materials for manufacturing low duty refractory castables for furnace backup and refractory mortar.

The energy expended in separating the entrapped metal from the spent refractory lining was evaluated using the Bond Work Index test. An industrial process design model was developed with METSIM software using Bond Work Index test data to summarize the cost benefits associated with the proposed recycling program for spent refractory linings.

## ACKNOWLEDGMENTS

I wish to express my deepest gratitude to my advisor, Dr. Kent D. Peaslee for providing me with an opportunity to pursue a master's degree in Missouri University of Science and Technology. His enthusiasm and constant support have motivated me to successfully complete my research work. His suggestions, guidance and personal attention have been constant source of encouragement.

I would like to thank my committee members, Dr. Von L. Richards and Dr. Jeffrey D. Smith for their time and effort in reviewing my progress. I would like to thank Dr. Simon Lekakh, for his immense support and guidance, without which this project would not have been possible.

I would like to thank Dr. Charles H. Rawlins, Dr. David Robertson, Todd P. Sander, William Peach, and Jared Teague for their continuous support. I would also thank William Headrick from Morco Refractories for his help and Eric Bohannon for his help in analyzing the X-ray diffraction data.

Finally, I would like to thank my parents, brother, and friends for their continuous support and care.

## TABLE OF CONTENTS

	Page
ABSTRACT.....	iii
LIST OF ILLUSTRATIONS.....	vii
LIST OF TABLES.....	ix
SECTION	
1. LITERATURE SURVEY .....	1
1.1. CONCEPT OF WASTE MINIMIZATION AND RECYCLING.....	1
1.2. REFRACTORY RECYCLING PRACTICES.....	3
1.2.1. MgO-C Refractories Recycling Practices.. ..	3
1.2.2. Recycling of Magnesite and ZAS Refractory Bricks.....	3
1.2.3. Recycling of 70% Al <sub>2</sub> O <sub>3</sub> Spent Refractory. ....	4
1.2.4. Recycling of Spent Magnesia-Chrome Refractories.. ..	4
1.3. COPPER BENEFICIATION METHODS.....	5
1.3.1. Solvent Extraction and Electrowinning (SX/EW).....	5
1.3.2. Segregation Roasting.....	6
1.3.3. Crushing and Grinding.. ..	7
1.4. OUTLINE OF THE PROJECT .....	8
2. EXPERIMENTAL STUDY OF COPPER RECOVERY .....	10
2.1. EXPERIMENTAL PROCEDURE.....	10
2.1.1. Characterization of Spent Linings.....	10
2.1.1.1 Macro-characterization .....	11
2.1.1.2 Micro-characterization.....	13
2.1.2. Acid Leaching Procedure.. ..	14
2.1.3. Metal Liberation by Comminution.....	17
2.2. RESULTS AND DISCUSSION.....	19
2.2.1. Copper Content in Penetrated Layer.. ..	19
2.2.2. Brass Morphology in Spent Refractory Linings.....	20
2.2.3. Total copper in Lining Samples. ....	23

3. PROCESSING OF NEW REFRACTORY CASTABLES USING SPENT LINING .....	29
3.1. BACKGROUND ON CASTABLES.....	29
3.1.1. Particle Size Distribution.....	29
3.1.2. Curing and Firing.. .....	31
3.1.3. Processing of Castables from Spent Refractory.....	32
3.2. EXPERIMENTAL PROCEDURE .....	33
3.3. RESULTS AND DISCUSSION.....	35
4. INDUSTRIAL PROCESS DESIGN AND SCALE UP.....	39
4.1. PROCESS DESIGN .....	40
4.1.1. Bond Work Index Test Procedure .....	41
4.1.2. METSIM Design.....	44
4.2. BOND WORK INDEX TEST RESULTS.....	42
4.3. METSIM PROCESS DESIGN .....	44
4.4. RESULTS AND DISCUSSION.....	48
5. CONCLUSIONS .....	52
6. FUTURE WORK.....	54
APPENDICES	
A. TABULATED RESULTS OF TOTAL COPPER FOR EACH LINING TYPE ....	55
B. MATERIAL DATASHEET FOR TYPE C VIRGIN REFRACTORY .....	61
C. PARTICLE SIZE DISTRIBUTION FOR PROCESSING NEW CASTABLES....	63
D. METSIM HELP FILES .....	65
BIBLIOGRAPHY.....	69
VITA .....	72



## LIST OF ILLUSTRATIONS

Figure	Page
2.1. Macro photos of samples from six types of refractory linings, A through F.....	12
2.2. SEM micrographs of samples from a) type C castable refractory at the metal-ceramic interface illustrating that there is physical wetting of ceramic matrix by brass and b) type A rammable refractory illustrating particles (~ 1µm) wetting the ceramic matrix. ....	13
2.3. Test results for two different acid concentrations to develop acid leaching procedure. ....	15
2.4. XRF calibration curve generated from copper standard solutions.....	16
2.5. Jaw crusher showing the open side gap setting and closed side gap setting.....	17
2.6. Flow chart for developed crushing and grinding circuit.....	18
2.7. SEM micrographs of C type refractory showing a) type 1 - elongated brass strips b) type 2 - brass particles (~ 1µm) wetting the refractory matrix and c) type 3 - thin metal foils.....	20
2.8. Macro-photos of a) D type refractory and b) new D2 type refractory samples.....	22
2.9. a) Particle size distribution of crushed samples (error ~7%) and b) distribution of total copper content at each particle size fraction in crushed lining (error ~8%)...	23
2.10. Cumulative copper distributions after crushing for all the lining samples at each specified size fraction (error ~10%). ....	25
2.11. Average copper present in test samples of different refractory types.....	26
2.12. XRD patterns generated for samples from a) D type refractory b) D2 type refractory c) D2 type refractory indicating the presence of spinel phase.....	27
3.1. Crucible mold design for processing castables from virgin and crushed spent lining.....	32
3.2. a) Porous castable prepared from virgin castable mix b) dense castable prepared from normalized castable mix of type C refractory.....	33
3.3. Particle size distribution for virgin mix and normalized virgin mix plotted with cumulative percent finer than (CPFT) against size fraction in micrometers.....	34
3.4. Macro photographs of all four castables a) before firing b) after firing c) after testing for 48 hours.....	36
3.5. Macro photograph of castable 4 indicating the location of all cross-section samples. ....	37

3.6. Stereoscope cross-section images from hot face to cold face of a) castable 1 – virgin blend b) castable 2 - '90-10' blend c) castable 3 – '50-50' blend and d) castable 4 – blend of crushed spent lining.....	38
3.7. Optical micrographs of hot face of four types of castables showing no metal penetration after 48 hours of testing a) Castable 1, b) Castable 2, c) Castable 3, d) Castable 4. ....	39
4.1. The net grams per revolution plotted against period number showing steady state for fifth, sixth and seventh period.....	43
4.2. The particle size distribution of feed, circulating load and product .....	44
4.3. METSIM grinding circuit (Jaw crusher model) for calculation of comminution energy for refractory lining showing mass flow rate and P80 for respective streams.....	45
4.4. Process flow chart developed in METSIM for double stage jaw crusher.....	47
4.5. Comparison of three models based on the energy expended to crush to a specified product 80% passing .....	49
4.6. Particle size distributions obtained from double stage (DS) jaw crusher model compared with optimal distribution .....	49

**LIST OF TABLES**

Table	Page
2.1. Chemical composition of different linings. ....	10
2.2. Macro-characterization results for each refractory type. ....	11
2.3. Copper content in penetrated layer of test samples. ....	19
2.4. Estimated % copper in the entire linings. ....	21
2.5. Copper distributions in the crushed refractory linings.....	26
3.1. Blend compositions for different castables.....	35
4.1. The BWI test results for crushed lining.....	43
4.2. Power Draw and Dimensions for the Process Design and Scale up model.....	46
4.3. Cost savings for different recycling alternatives.....	51

## **1. LITERATURE SURVEY**

The concept of waste minimization and recycling has gained importance in modern research with emphasis shifting toward resource conservation and environmental protection. Approximately three million tons of spent refractory materials are generated annually in US by the ferrous, non-ferrous, and glass industries [1]. Spent refractory linings constitute a major percentage of the industrial waste generated by metal manufacturing plants. The major constituents of refractory linings are silicates, aluminates, magnesia, zirconia, carbides, oxides, fused materials and various combinations thereof. The blend for each refractory lining is prepared specifically based on performance resulting in the use of special additives, often without concern for recycling.

### **1.1. CONCEPT OF WASTE MINIMIZATION AND RECYCLING**

The most effective method of waste minimization is to generate less waste [2]. This can be achieved by improving the life of refractory materials and also by applying different refractories in the different zones of the furnace to increase effective refractory utilization. Recycling spent refractory linings in the ferrous industry has been extensively studied and corresponding recycling procedures have been established. The introduction of slag splashing in steelmaking furnaces has extended the life of refractories wherein the viscous slag is splashed on the sidewalls of the furnace at the end of the blow forming a protective adhesive layer. However, due to process differences, similar techniques cannot be used in the non-ferrous industry.

The most common reasons for landfilling spent refractories are the high costs associated with the re-use of the spent linings, the perceived poor quality of re-used materials due to the presence of contaminants, and the low cost of space in a landfill [2]. The value of the material recovered in the recycling process has a major impact on recycling efforts. The reduction in the quality of the material and also the added costs for recycling inhibits the implementation of large scale recycling programs. The recycling program is generally based on factors such as binding materials, possible contaminants,

hazardous components (such as hexavalent chrome or lead) and beneficiation costs. A lack of understanding of the economics associated with refractory recycling in the non-ferrous industry contributes to most users landfilling rather than recycling because recycling processes are not perceived as adding economic benefit.

The factors impacting refractory recycling are the frequency of generation, economics of beneficiation, volume of refractories landfilled, value of recovered components, the type of refractory, and the mix of lining materials. The type of refractory was identified to play a role because monolithic refractories are difficult to handle in comparison with the refractory bricks as monolithics are large structures anchored to the base of the furnace.

Legislative regulations have classified certain materials like lead and hexavalent chromium as hazardous waste. Hazardous waste is banned from landfills, leading to the development of recycling and recovery techniques for chromium oxide containing refractories [1]. However, for non-hazardous waste, the economic incentive associated with the recycling process is the main driving force for industries to recycle the generated waste. The economic benefits associated with the re-use of the spent refractories and recovery of valuable byproducts make recycling process more economical than landfilling. Possible applications identified [1-4] are soil conditioner, slag conditioner, components in cement aggregates, landscape material and grog in ceramic materials.

The initial step in developing a typical refractory recycling process is sorting the materials based on the type of refractory [3]. Sorting allows the segregation of similar types of refractories for more economical beneficiation. After sorting, the spent refractory linings are sampled and characterized. Characterization helps to identify metal penetration and erosion-corrosion of the refractories due to high temperature wear and exposure to molten metal. Visual examination at the macro level identifies changes in the refractory after extended use and characterization using tools like microscopy, chemical analysis, x-ray diffraction provide insights to possible beneficiation techniques [2, 3].

Crushing and grinding followed by screening facilitates ease of handling and also helps in liberation of recoverable products [4]. An appropriate separation technique or techniques liberate re-usable byproducts and eliminate impurities. Magnetic separation is effective for magnetic byproduct or contaminant like steel/iron. Solvent extraction and

electrowinning (SX/EW) are common separation techniques used for non-magnetic contaminants.

## **1.2. REFRACTORY RECYCLING PRACTICES**

As a background to previous recycling efforts for spent refractory linings, the recycling of spent MgO-C [5], Magnesite-ZAS (zirconium aluminum silicate) bricks [6], Al<sub>2</sub>O<sub>3</sub> refractories [7, 8] and magnesia-chrome refractories [9-11] are briefly described.

**1.2.1. MgO-C Refractories Recycling Practices.** The MgO-C and MgO refractories are used extensively in EAF steelmaking. The recycled product can be used as gunning mix to repair cracks and crevices in the highly erosive zones of the furnace. MgO is added to slags to prevent furnace lining wear during steelmaking. Recycled MgO can be used as a potential slag conditioner [5].

The recycling program established by Kwong and Benett [5] established a model to optimize the MgO content in foamy slag and to determine the optimum amount of MgO to be added. The spent refractory chunks were crushed and optimum aggregate size was determined to control the dissolution rate of MgO. To increase dissolution rates in slag, a 4-5mm aggregate size was proposed.

**1.2.2. Recycling of Magnesite and ZAS Refractory Bricks.** Magnesia is extensively used in ferrous industries due to its resistance to FeO rich slags. Al<sub>2</sub>O<sub>3</sub>, TiO<sub>2</sub> and ZrO<sub>2</sub> are added to improve the mechanical properties of magnesia [6]. The bonding between magnesia grains can be improved by increasing the CaO/SiO<sub>2</sub> molar ratio to 2.0.

Recycling magnesite and ZAS bricks was done by Othman and Nour [6] and they investigated the properties of magnesite refractory brick with recycled ZAS additions (1-10 wt. %). The crushed bricks of spent magnesite and ZAS refractories were tested for refractoriness under load (RUL) and thermal shock resistivity. Refractoriness under load determines the deformation point of the refractory under constant load. A 5% ZAS addition increases the thermal shock resistivity and refractoriness under load for the new bricks and resulted in higher shock resistance and refractoriness than that of the pure magnesia bricks [6].

**1.2.3. Recycling of 70% Al<sub>2</sub>O<sub>3</sub> Spent Refractory.** Brass companies use neutral refractories like alumina silicates in melting furnaces. Typically most of the companies landfill their refractories. Characterization of spent refractories is a primary step for refractory beneficiation. It allows selective separation of desired and undesired materials thereby saving time and cost of analysis. In the study by Kwong, Benett and Collins [7], refractory samples representative of different areas of the furnace were characterized using scanning electron microscopy (SEM) and energy dispersive X ray analysis (EDAX/EDS). The SEM results provided the basis for liberation of the penetrated layer and recycling of the crushed lining.

The alumina silicate refractories have gained importance to replace magnesite-chrome refractories [8] so that hexavalent chromium formation can be avoided and the spent refractory linings can be landfilled as non-hazardous waste. Magnesite-alumina and alumina silicates were considered as suitable replacement owing to their good erosion-corrosion properties.

**1.2.4. Recycling of Spent Magnesite-Chrome Refractories.** Magnesite-chrome refractories have been widely used in copper smelting furnaces until they were identified as hazardous waste. In one study, the spent refractory linings were subjected to water leaching to remove sulfates. The sulfur ion removal also effectively dissolves chromium and the remaining residue was re-usable [8].

Several attempts [9-11] have been made to find suitable replacements for magnesite-chrome refractories. Magnesite-alumina based refractories seem to have the potential to replace magnesite-chrome in copper smelting furnaces. If copper penetration is significant, then liberation of the penetrated copper could add economic benefit. Copper and copper alloys have a tendency to penetrate into refractory lining and appropriate material blends for longer service life of refractories in copper smelting furnaces need to be developed.

In recycling studies [9-11], copper contaminated bricks from copper smelting furnaces were ground and subjected to leaching or flotation and the residue was re-used [9-11]. Important considerations during recycling were that the end re-usable product not contains contaminants and the beneficiation costs should not exceed the costs for

transportation and landfill. The various copper beneficiation techniques have been described in the next section.

### **1.3. COPPER BENEFICIATION METHODS**

The continuous wear and erosion-corrosion of refractories facilitate metal penetration into the refractory filling cracks and pores. The recovery of entrapped metal can improve the economics of recycling. Metal penetration is inevitable in melting furnaces; however the mechanism of penetration can assist in recovering the entrapped metal. There are several methods of recovering copper from spent refractory linings including solvent extraction, segregation roasting and simple comminution techniques such as crushing and grinding.

**1.3.1. Solvent Extraction and Electrowinning (SX/EW).** Leaching is the first step in solvent extraction and electrowinning of copper. Leach solution is generally pure acid or mixed acid solution in which copper is dissolved and the solution is then subjected to SX/EW.

Solvent extraction is the process in which copper contained in the low-acid leach solution is extracted [12] by an organic reagent and then re-dissolved in highly concentrated acid solution which is used as an electrolyte in electrowinning. The organic layer after extraction is re-used. The leach solution after two extractions would still be rich in copper. This is called raffinate. The raffinate is recycled back to leach liquor for re-extraction.

Electrowinning is a copper liberation step in which a lead containing anode and pure sheet copper cathode and leach solution (electrolyte) complete the electric circuit and copper from electrolyte is deposited on the cathode. The entire SX/EW process is an economical process for copper extraction from ores. However, as a preparatory step, the copper ores or copper rich material are first subjected to crushing and grinding since fine particles have more surface area and hence are more suitable for dissolution in low acid solution.

Various processes were developed relative to the value of ore/mineral, the concentration of metal, the cost of the raw materials, and energy consumed for crushing



and grinding for fine particle size matrix. The successfully recycling practices for recovering copper from secondary sources include leaching and electrochemical recovery of copper from printed circuit board scrap [14]. However due to the presence of various metal parts, the leaching process for copper recovery from printed circuit board scrap was complicated. Selective extraction of copper was done by using aqueous nitric acid solution at various concentrations and the process was optimized to recover copper and other precious metals. Mechanical recovery through crushing and grinding is also possible but requires high energy.

Solvent extraction was suitable when two or more precious metals had to be recovered and separated. Nitric acid in conjunction with sulfuric acid was generally used in copper recovery processes from highly concentrated secondary sources. Molybdenum and copper recovery and separation are achieved by a solvent consisting of sulfuric acid and sodium nitrate [15].

The heap leaching of oxide copper ores with copper recovery from the SX/EW process is considered to be a low cost method. The typical operating cost is based on the value of the ore, mining costs, energy consumption for comminution, acid requirements, copper recovery and operating power costs. The potential drawbacks are SO<sub>2</sub> emissions and sulfuric acid concentration. Hence, ammonia based and nitric acid based leach solutions are being used as alternatives.

Crushing and grinding must be optimized as size reduction to fine particle size of the mineral lowers the metal recovery and iron and sulfur precipitation may occur. Crushing to ultra fine particles also increase the operating costs.

**1.3.2. Segregation Roasting.** Segregation roasting was developed to recover copper from crushed magnesite bricks by J. Bear and J.F. Moresby [16]. The preliminary step was to crush and grind the material down to a product screened with 14 mesh opening. The coarse 14 mesh oversize containing 72% copper was directly fed back to the smelter for copper recovery without further treatment and the undersize 14 mesh particle size fractions were analyzed for segregation roasting.

The oxidation roast pre-treatment was to allow copper sulfides and copper metal in magnesite bricks to segregate as a mixture of sulfates and oxides. L.J. Bear and J.F. Moresby [16] found that at 700° C pre-roast temperature, copper successfully segregated

as a sulfate. Salt and carbonaceous material was added to reduce the copper sulfate to copper. The segregation temperature was found to be optimum at 660 °C, which was considerably lower in temperature than the predicted range of 750 °C – 850 °C [16]. The process can recover approximately 85%-90% of copper from the refractory bricks.

Pyrometallurgical processes have several advantages over hydrometallurgical processes. The energy consumption is lower for pyro-derived processes and the process of recovery is simple as compared with the hydrometallurgical processes. Precious metal recovery through roasting is more efficient than leaching as the recovery from leach residue is a complex process.

**1.3.3. Crushing and Grinding.** Crushing and grinding are the basic operations under comminution techniques. Comminution is breaking down of large chunks of material into smaller fractions by applying compressive forces and is typically the first step in the recycling process of spent refractory lining as other recovery processes cannot handle large chunks of material.

The metal recovery through simple crushing and grinding operations can facilitate an economic basis for recycling materials. Crushing applies compressive forces and literature [17] indicates that copper is more ductile with more strain at ultimate stress than materials like steel, zinc, lead and silver and for more than brittle bricks. This implies that copper recovery through crushing and grinding is more feasible other recovery of other metals.

The initial attempts to recover copper from electronic scrap through simple crushing and grinding operation have been made by W. Hui, G.G. Hua and Q.Y. Feng [18] and a jaw crusher was used in conjunction with a roll and gyradisc crusher and the individual size fractions were analyzed after crushing to estimate the metal recovery from the printed circuit board (PCB) scrap.

The printed circuit board scrap is quite complex due to the presence of many metallic components, plastics and ceramics. The evaluation of crushing and grinding performance indicated that compressive type crushers such as jaw crushers, roll crushers and gyradisc crushers cannot handle the scrap efficiently; however an impact crusher comminutes the scrap better.

Crushing and grinding operations can be effective depending upon the mechanism of metal penetration in secondary sources. Crushing would segregate the metallic value of the PCB scrap thereby recovery is possible by density separation techniques. However, if the recovery rates for crushing and grinding are higher, it can be developed into an effective metal recovery process. This is due to the fact that the process avoids the use of complex leach solutions, and eliminates processing steps adding economic benefits to the recycling program.

#### **1.4. OUTLINE OF THE PROJECT**

The literature review indicates that characterization of spent refractory samples to understand the metal penetration mechanism and prediction of possible liberation techniques is critical to evaluate and design recycling process.

Segregation roasting was not considered for the present study due to lower metal concentration in the spent refractory linings and also because of the possibility that the beneficiation expenses might exceed the costs of recycling. Acid leaching was selected as a possible beneficiation method because of lower operating costs involved in liberating copper but involves secondary metal recovery steps. However, the benefits of recycling can be maximized if simple crushing and grinding operation would liberate high quality metallic product thereby eliminating secondary recovering processes.

The main objective of the present project is to study the feasibility of metal liberation entrapped in spent refractory lining by crushing and grinding and recycling of refractory into new products. The project focuses on the following:

- Metal recovery by crushing and grinding operation, followed by selective screening.
- Recovery of the crushed lining and prepare re-usable castables for low duty applications.
- Bond Work Index testing to evaluate the energy requirements for crushing and grinding operations and provide possible suggestions for industrial process design.

- Industrial process design and scale up for the recovery process and recommendations based on energy calculations using Bond Work Index and METSIM software.
- Analyze the cost benefits involved in recovery of materials from spent linings and provide cost based recommendations.

## 2. EXPERIMENTAL STUDY OF COPPER RECOVERY

### 2.1. EXPERIMENTAL PROCEDURE

A brass producer uses six types of high alumina and alumina silicate refractories for copper melting, four in the inductors, one in the furnaces and one in the troughs. Spent refractory linings from the melting furnaces represent 80% of the annual tonnage of refractories that are landfilled by this company. Spent refractory samples from the six different refractory types were obtained from the brass producer and characterized for metal content and size and shape of the trapped metal. Samples were acid leached initially and at various stages of the recycling process to determine the metal content. Various crushing and grinding techniques and sequences were used to liberate the metal and facilitate separation of the metal from the refractory.

**2.1.1. Characterization of spent linings.** Six different types of refractory used for the various applications in the brass melting process were designated as refractory A, B, C, D, E, and F as summarized with chemical compositions in Table 2.1.

Table 2.1. Chemical composition of different linings.

Type	Usage	Chemical Composition (wt. %)				
		Alumina	Silica	Silicon Carbide	Titania	Magnesia
A	Inductors	71.1	9.60	16.0	2.4	NA
B	Inductors	91.9	2.50	NA	NA	4.4
C	Inductors	76.3	7.10	11.6	3.0	NA
D	Furnaces	61.5	33.0	0.00	2.0	NA
E	Troughs	95.0	NA	NA	NA	NA
F	Inductors	70.8	10.0	6.80	2.3	NA

NA = not available

The chemical compositions were obtained from the material datasheets of refractory manufacturers provided by the brass producer. The alumina based refractories

were most likely prepared from bauxite ores. Types A and D are rammable refractories and type B, C, E and F are castable refractories. Inductors have varying amount of silicon carbide indicating that the refractories used in inductors are subjected to more corrosive environment than the furnaces. Troughs are lined with higher alumina refractory to withstand the abrasive conditions in the distribution channels. The representative lining samples were subjected to macro and micro-characterization to understand the nature of the metal penetration, the thickness of the hot face, and determine the nature of metal penetration.

**2.1.1.1 Macro-characterization.** The aim of macro-characterization was to analyze the hot face of the lining samples, its condition and provide a rough estimate of the thickness of the penetrated layer. The samples have distinct discoloration across the section indicating wear and erosion by the hot metal and also possible metal penetration. The thickness of discolored layer from hot face was measured and is defined as the penetrated layer (see Figure 2.1). Table 2.2 lists the thickness of the penetrated layer and the number of test samples analyzed. The macro photographs of the test samples (see Figure 2.1) show the penetrated layer separating the reacted region near the hot face from the passive region near the cold face of the spent linings.

Table 2.2. Macro-characterization results for each refractory type.

Description	Penetration of Samples	
	Number of samples	Average penetration (cm)
A	4	$2.9 \pm 0.7$
B	6	$4.0 \pm 1.1$
C	7	$3.5 \pm 1.3$
D	7	$1.0 \pm 0.4$
E	5	$0.7 \pm 0.3$
F	2	$0.7 \pm 0.5$

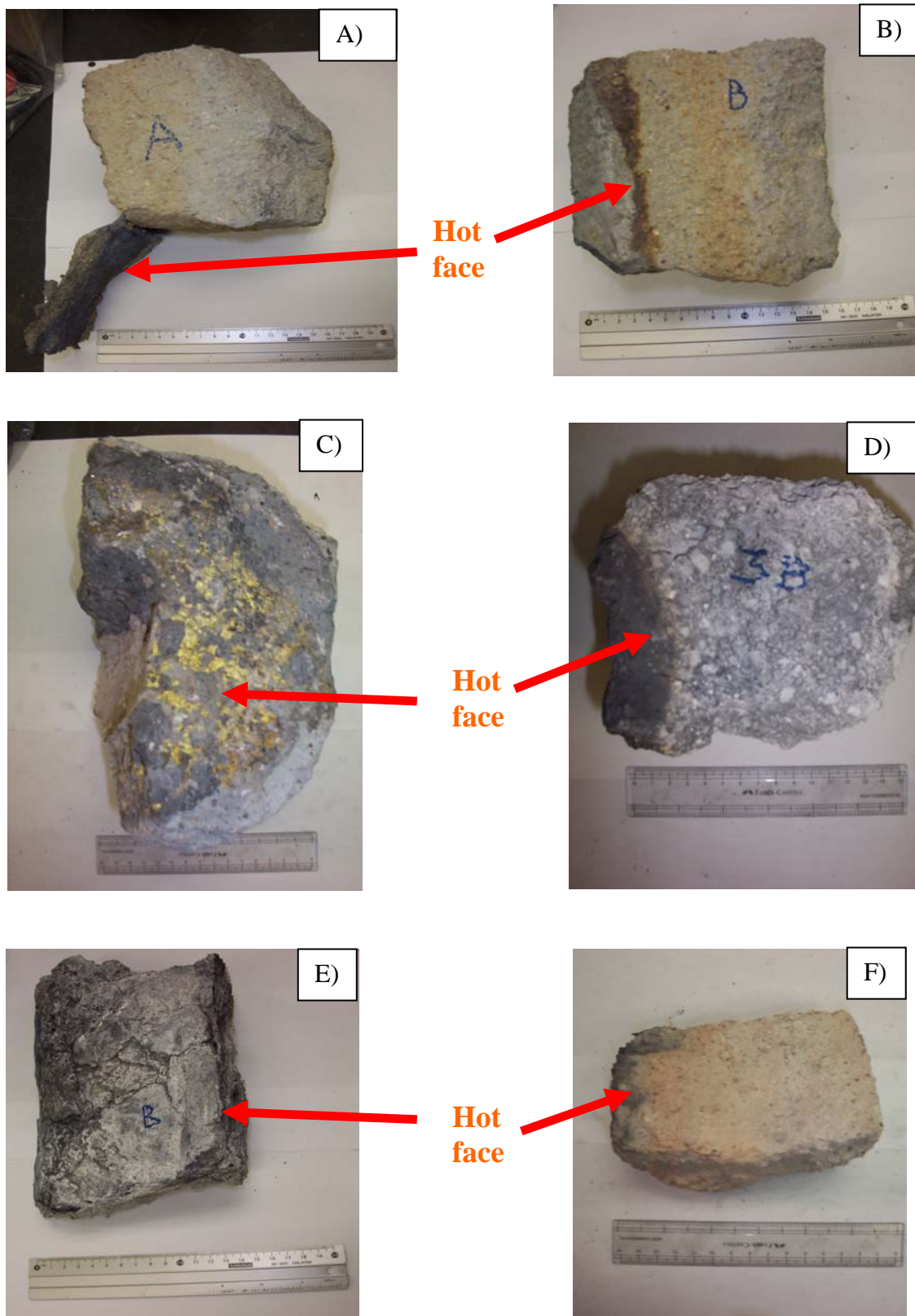


Figure 2.1. Macro photos of samples from six types of refractory linings, A through F.

The hot face in samples E and F do not appear to have high metal penetration and the thickness of hot face is much less when compared to the other refractory types (see Table 2.2). Since the penetration layer is not significant, copper content would be negligible possibly eliminating the refractories E and F from being recycled. Refractories A, B, and C had significantly more penetration than the other refractory types. Since all three refractory types were used in inductors, it can be inferred that the inductor linings would have higher metal content than the lining used in furnaces and troughs. The melting furnaces used by the brass producer are channel induction furnaces rather than coreless. The channel induction furnace consists of steel shell lined with refractory materials and an inductor attached to it. A channel connects the main body with the inductor. Therefore, the advantage of channel induction furnaces is that the A, B and C inductor linings can be individually detached and recycled.

**2.1.1.2 Micro-characterization.** The penetrated layer for one sample from the type C castable type refractory and one sample from type D rammable type refractory were cross-sectioned and examined with Scanning Electron Microscopy (SEM) (see Figure 2.2) Hitachi S570.

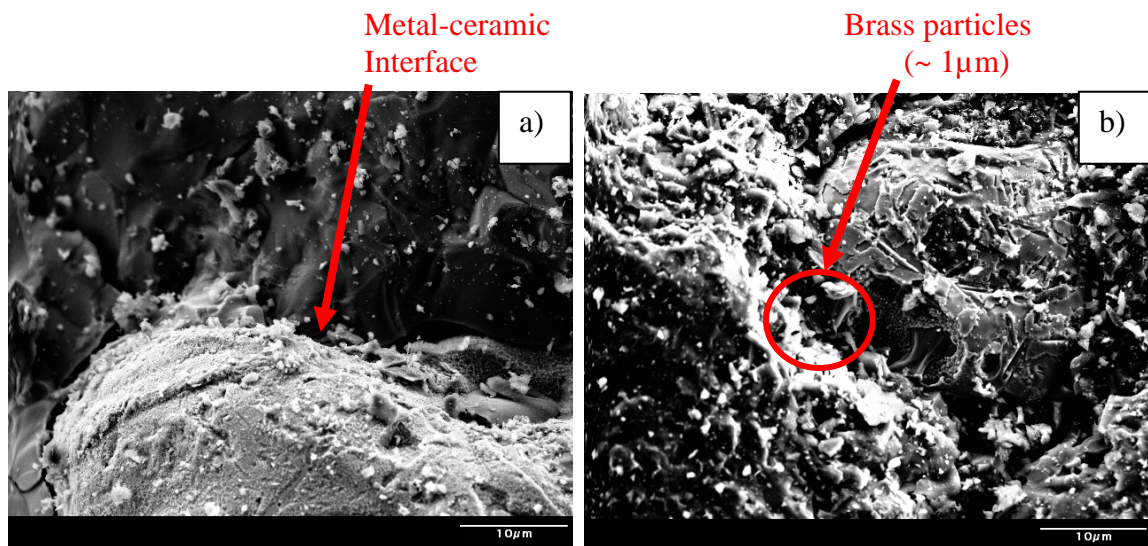


Figure 2.2. SEM micrographs of samples from a) type C castable refractory at the metal-ceramic interface illustrating that there is physical wetting of ceramic matrix by brass and b) type A rammable refractory illustrating particles ( $\sim 1\mu\text{m}$ ) wetting the ceramic matrix.



In Figure 2.2, metal penetration into the cracks developed in the refractory was observed for both rammable and castable samples. The absence of an intermediate layer at the metal-ceramic interface in the micrographs (see Figure 2.2) of samples from C and A type refractories indicate that there is no reaction between the entrapped metal and the ceramic matrix. Brass particles ( $\sim 1\mu\text{m}$ ) were also identified using Energy Dispersive Spectroscopy (EDS) analysis.

The brass penetrated into the cracks developed in the refractory lining forming elongated strips. Since the metallic strips are physically wetting the refractory matrix, it is expected that crushing and grinding technique could liberate the strips and subsequent screening can separate the liberated brass strips from the lining samples. However, for the crushing and grinding procedure to yield maximum benefits, it is necessary to evaluate the total copper present in the penetrated layer. Acid leaching was used to dissolve all of the copper in the lining followed by x-ray fluoroscopy to analyze the total copper content in the lining samples.

Since it was difficult to analyze the total brass content in the spent linings, copper content was analyzed using acid leaching procedure and XRF analysis. The brass strips that are crushed and screened are weighed and multiplied by 0.9 to convert the brass content to copper content. The estimation that brass contains 90% copper was based on the information supplied by the brass producer. The total metal content (brass) in the spent linings is 1.1 times the analyzed copper content in all the results provided in the subsequent sections.

**2.1.2. Acid Leaching Procedure.** Separating and recovering the metal entrapped in the refractory can provide economic benefits if the revenues from the recovered materials and products exceeds the cost to process. The percentage of metallic content and the type of metal are major factors determining the overall economic feasibility of the recycling program. Hence, determination of copper content in the test samples was critical.

An acid leaching procedure was defined by sequence of steps:

- Standard solutions of 2.5g, 5g, 7.5g and 10g Cu/300ml of solution were prepared to calibrate X-Ray Fluoroscopy (XRF) and a calibration curve was developed for further analysis.

- Cross sectioned lining sample using wet diamond saw and multiple cuts to obtain  $10 \pm 2$  grams of sample from the penetrated layer.
- Crush the sample using cup and pestle (10 grams).
- Add crushed sample to 300 ml of acid solution with 10 %  $\text{HNO}_3$  and 10 %  $\text{H}_2\text{SO}_4$  in a 500ml beaker.
- The beaker is placed on magnetic stirrer and stirred for 24 hours at room temperature.
- The test solutions are analyzed using XRF and intensity values plotted on the calibration curve to determine the copper content in solution.

The concentration of leach solution was optimized by trial and error. The first trial used 5%  $\text{HNO}_3$  and 5%  $\text{H}_2\text{SO}_4$  and the second trial concentration of 10%  $\text{HNO}_3$  and 10%  $\text{H}_2\text{SO}_4$ . As illustrated in Figure 2.3, the trial with 5%  $\text{HNO}_3$  and 5%  $\text{H}_2\text{SO}_4$  acid concentration could not leach out all the copper present in the crushed sample for the first leaching experiment. The solid to liquid ratio in acid leaching is generally maintained at 1:6 [12] and hence, the acid concentration was increased to 10%  $\text{HNO}_3$  and 10%  $\text{H}_2\text{SO}_4$ .

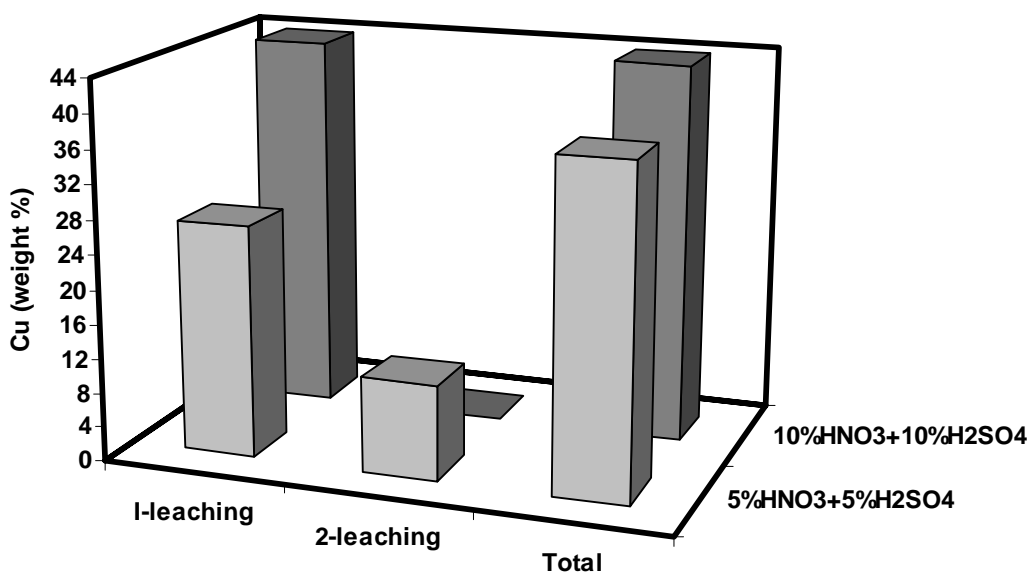


Figure 2.3. Test results for two different acid concentrations to develop acid leaching procedure.

When a small amount of copper dissolves, the overall concentration of the solution drops significantly and subsequent reaction is limited because of low strength of the overall solution. Hence the solution was supersaturated with the mixture of two acids which have different solubility limit for copper dissolution. Literature studies [12] reveal that nitrogen species dissolve copper rich aggregates better than the sulfur species; hence a combination of the two acids was considered for the acid leaching experiments (see Figure 2.4).

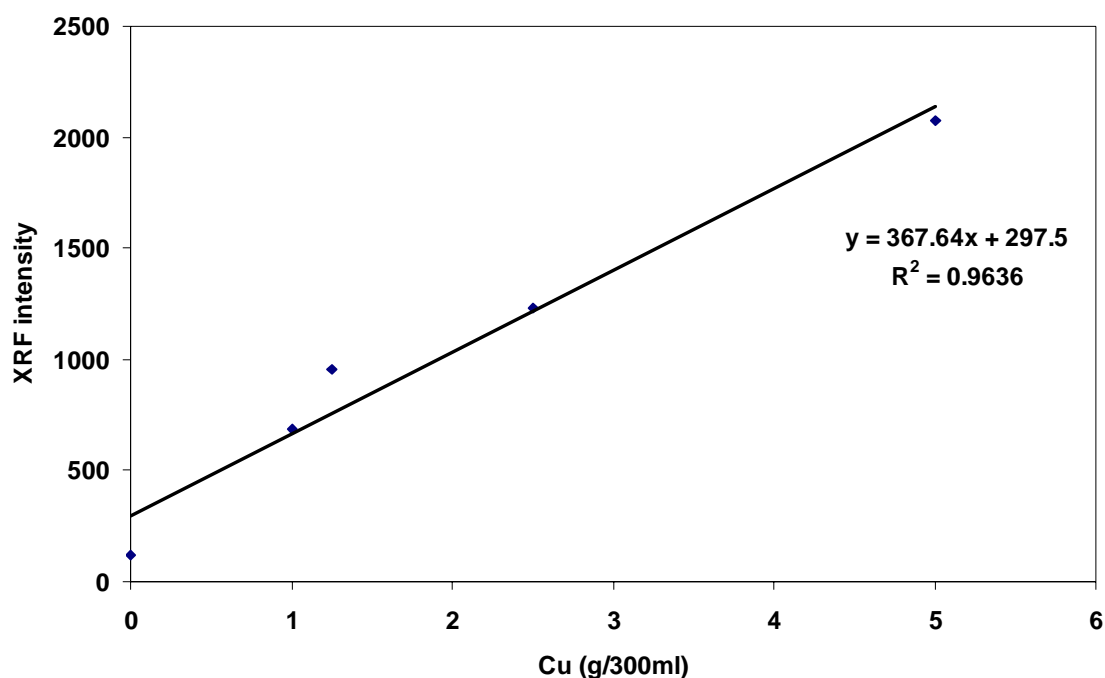


Figure 2.4. XRF calibration curve generated from copper standard solutions.

The X-ray fluorescence method determines the copper content in the solution. The XRF was first calibrated with a base leach solution with 0g copper and a calibration curve (see Figure 2.4) was obtained using standard solutions of 2.5g, 5g, 7.5g and 10g Cu/300ml of solution. The subsequent test samples were analyzed and superimposed on the calibration curve to calculate the percentage of copper present in the test samples.

**2.1.3. Metal Liberation by Comminution.** Based on the SEM analysis, brass penetrates through the cracks in the refractory and physically wets the refractory layer making a simple crushing operation possible to crack the brittle refractory layer while the ductile brass undergoes deformation thereby facilitating liberation by screening. A crushing procedure was developed at the laboratory scale with different gap settings for metal liberation, screening the elongated brass strips and subsequent estimation of copper retained in each particle fraction by acid leaching.

There are two gap settings for crushers defined as open side setting and closed side setting. The open side setting is the maximum gap or entrance for incoming feed material. The closed side setting is the gap for exit of crushed product (see Figure 2.5). For closed side setting in the laboratory jaw crusher, the maximum gap was 50mm and minimum gap was 5mm.

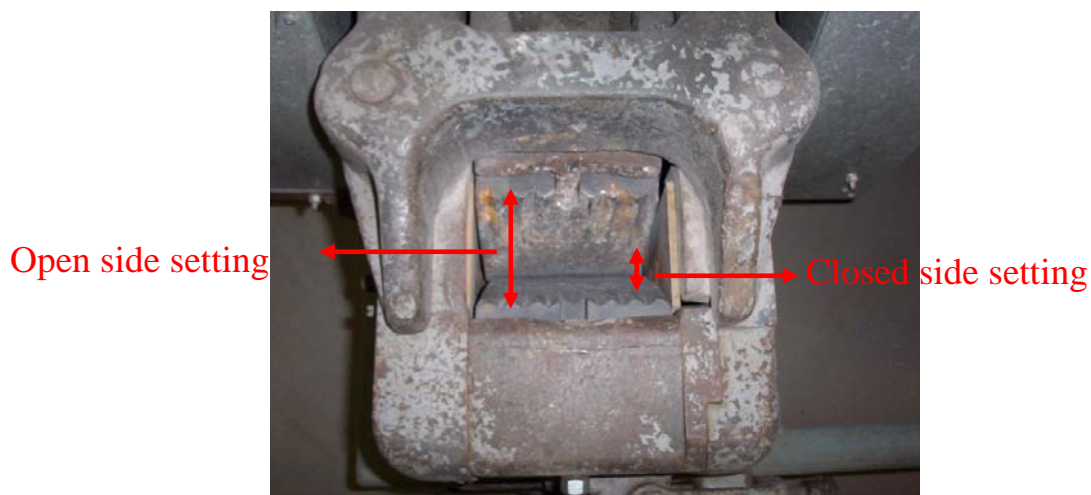


Figure 2.5. Jaw crusher showing the open side gap setting and closed side gap setting.

The crushing procedure described in the flowsheet (see Figure 2.6) was developed for the laboratory scale experiments 10grams of each size fraction of the crushed lining was acid leached and analyzed by XRF. The obtained copper values were extrapolated for the entire crushed lining (see Figure 2.9 b). The material retained at 16mm mesh size is the amount of brass that is effectively screened as strips.

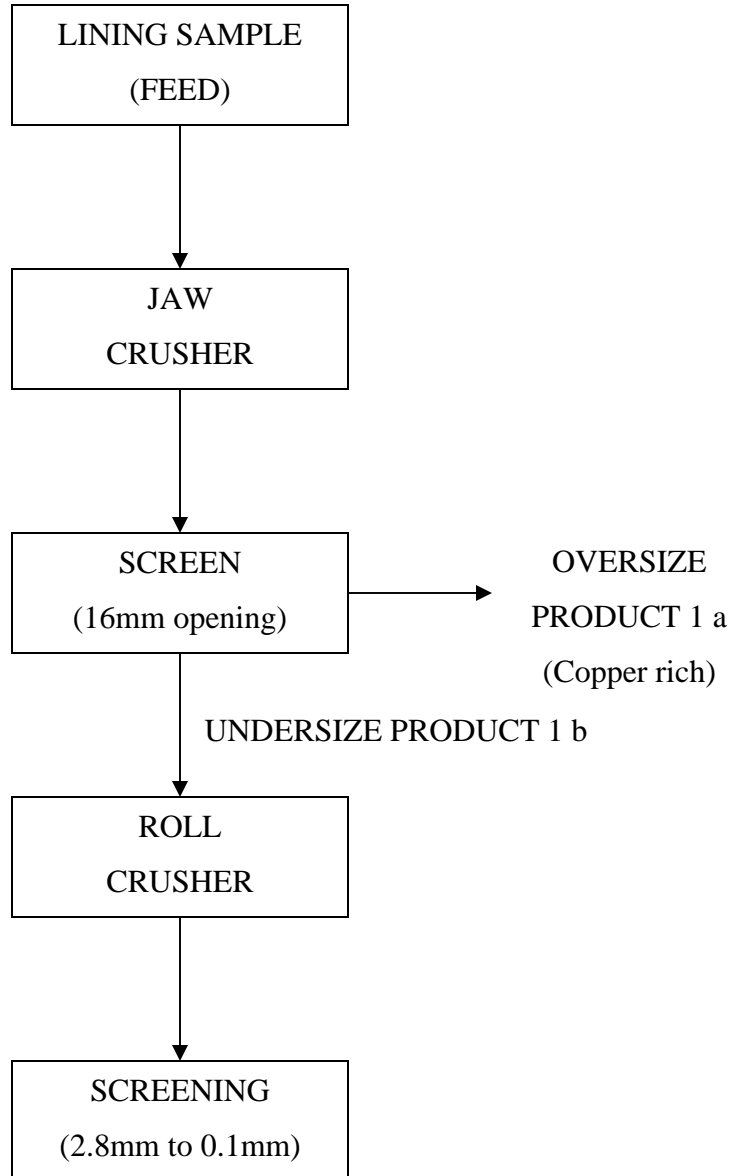


Figure 2.6. Flow chart for developed crushing and grinding circuit.

The laboratory crushing procedure for the spent lining samples is described.

- The lining samples were initially crushed with a hammer to accommodate the maximum open side setting (90mm) of the laboratory jaw crusher.
- The preliminary crushed material was then fed into jaw crusher with 50mm closed side gap setting for first stage of crushing.
- For the second stage jaw crushing, the closed side gap setting was 5mm.

- After the double stage jaw crushing, the product was sieved using a 16mm mesh opening to screen out the brass strips (product 1a).
- The remaining lining was fed into a roll crusher with a 2.5mm gap setting between the rolls for first stage roll crushing.
- For second stage roll crushing, the gap between the rolls was set at 0.7mm.
- The crushed product was sieved from 2.8mm through 0.1mm and a pan in a vibratable sieve shaker.
- The over-sized particles from each sieve were collected and 10 grams of sample representative of each size fraction was analyzed for copper content by the acid leaching procedure.

## 2.2. RESULTS AND DISCUSSION

**2.2.1. Copper Content in Penetrated Layer.** Two test specimens from each refractory were cut along the penetrated layer, and samples from penetrated layer were acid leached and analyzed for copper content using XRF. The results are summarized in Table 2.3.

Table 2.3. Copper content in penetrated layer of test samples.

Refractory type	Usage	Cu average (wt. %), in penetrated layer
A	Inductors for holders	$24.1 \pm 5.4$
B	Inductors	$4.5 \pm 1.8$
C	Inductors	$45 \pm 10$
D	Furnaces	$9.3 \pm 3.5$
E	Troughs	0
F	Inductors	$15.9 \pm 3.3$

The refractory type 'E' used for distribution channels did not appear to have any metal penetration although the samples appeared to have undergone wear, confirming the observations made in the macro-characterization and hence was not the focus for further studies. Although the 'F' type refractory had significant metal penetration it was also discarded from further studies due to the fact that the brass company did not have sufficient samples for analysis. Samples from refractory type A and C have significant metal penetration and hence these refractories are considered as potential materials to be recycled.

**2.2.2. Brass Morphology in Spent Refractory Linings.** The product from the crushing operation was analyzed for brass morphology using SEM. Three types of brass morphology were identified in the spent linings (see Figure 2.7).

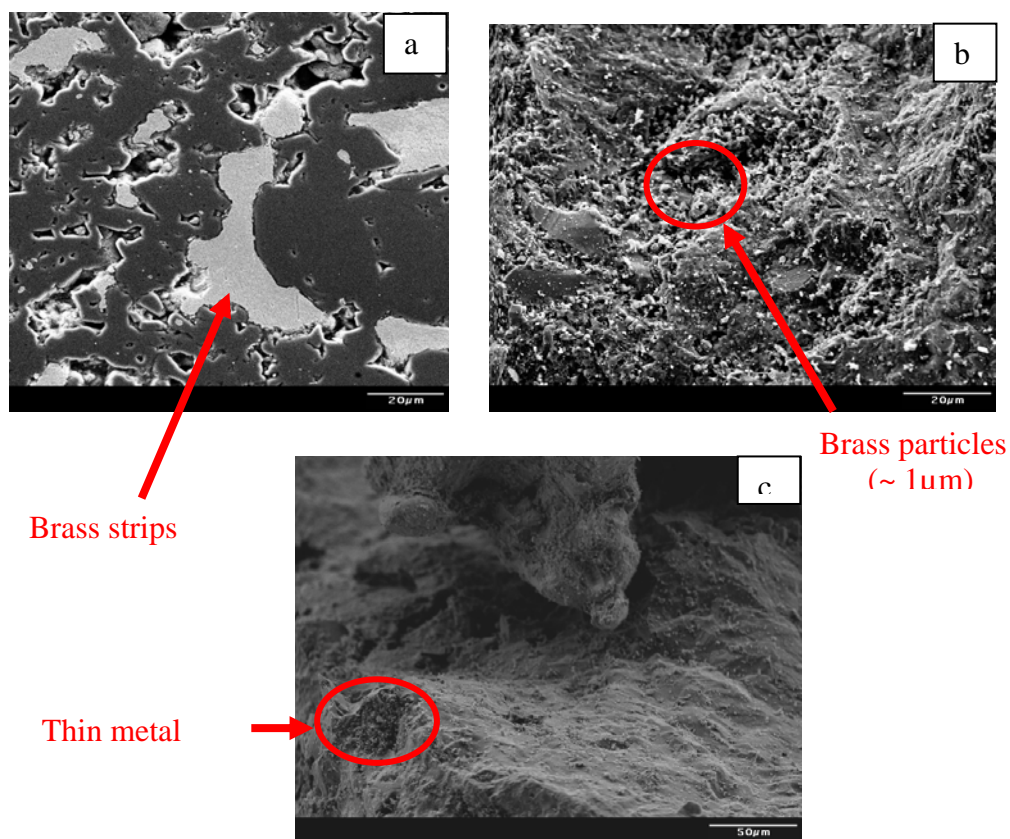


Figure 2.7. SEM micrographs of C type refractory showing a) type 1 - elongated brass strips b) type 2 - brass particles ( $\sim 1\mu\text{m}$ ) wetting the refractory matrix and c) type 3 - thin metal foils.

Metal penetration is inevitable in melting operations. However, the extent of penetration determines the economic feasibility of recycling. The extent of metal penetration cannot be observed by chemical analysis or X-ray diffraction. SEM studies of the samples from spent linings predict the extent of metal penetration.

Brass penetrates into the cracks of the refractory lining samples forming elongated copper strips. The metallic strips that are formed determine the extent of metal penetration into the refractory lining. The brass strips defined as type 1 can be recovered by simple crushing and grinding followed by mechanical separation by screening. Brass particles wetting the monolithic refractory are defined as type 2 and thin metal foils attached to the refractory particle are defined as type 3. The type 2 and type 3 can only be recovered by chemical leaching.

The characterization of the entire lining samples would help to estimate the total copper that can be liberated from the spent linings. Table 2.4 summarizes the characterization results for entire lining samples.

Table 2.4. Estimated % copper in the entire linings.

Refractory type	Annual % of refractory landfilled	Cu average (wt. %) in penetrated layer	Average thickness of Penetrated layer (cm)	Average lining sample width (cm)	Estimated Copper in linings (wt. %)
A	2.3	24.1 ± 5.4	2.9 ± 0.7	12.2 ± 2.2	6
B	1.0	4.5 ± 1.8	4.0 ± 1.1	8 ± 1.6	2.2
C	9.8	45 ± 10	3.5 ± 1.3	26 ± 2.5	6
D	81.7	9.3 ± 3.5	1.0 ± 0.4	13 ± 0.9	0.8
E	2.7	0	0.7 ± 0.3	4.2 ± 0.4	-
F	2.5	15.9 ± 3.3	0.7 ± 0.5	4.5 ± 0.3	2.4

The estimated percentage of copper was calculated from the total copper present in the penetrated layer and extrapolating the results for the entire lining sample. The



estimated copper percentage was used as a basis for further studies. The refractories used in A, B and C inductor furnaces show significant metal penetration and are favorable for recycling. However, these linings only represent ~14% of the total spent refractories which is comparatively less significant than the type D refractory which represents ~80% of the material landfilled. Although type F refractory samples were not considered for further studies because of insufficient samples for analysis, the characterization results indicate significant metal penetration and it could be a potential material to be recycled.

The type D refractory appears to have a much lower metallic content based on the characterization results from Table 2.4. However, ~80% of the annual refractory landfilled constitutes type D refractory linings. Therefore, new samples of type D refractory were collected from the brass producer to better represent the material. The new samples were designated as D2 and were macro-characterized for thickness of penetrated layer. Visual examination of samples from D2 type refractory indicate presence of brass strips (see Figure 2.8) with average thickness of penetration of  $3.9 \pm 0.4$  cm indicating the possibility of higher metal penetration than samples from D type refractory.

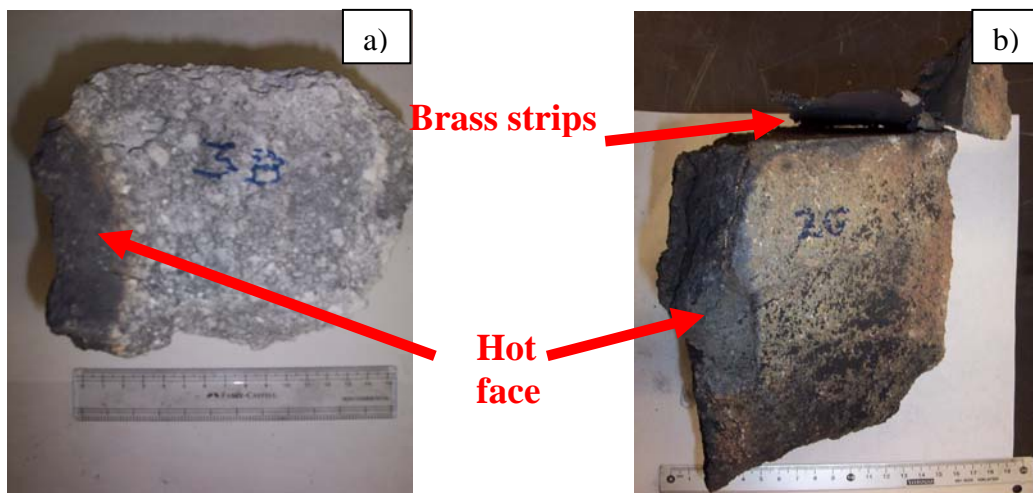


Figure 2.8. Macro-photos of a) D type refractory and b) new D2 type refractory samples.

**2.2.3. Total Copper in Lining Samples.** Two lining samples from A, B, C, D and D2 type refractories were crushed, leached and analyzed for total copper content using XRF (Figure 2.9). The tabulated test results and individual analysis are provided in Appendix A.

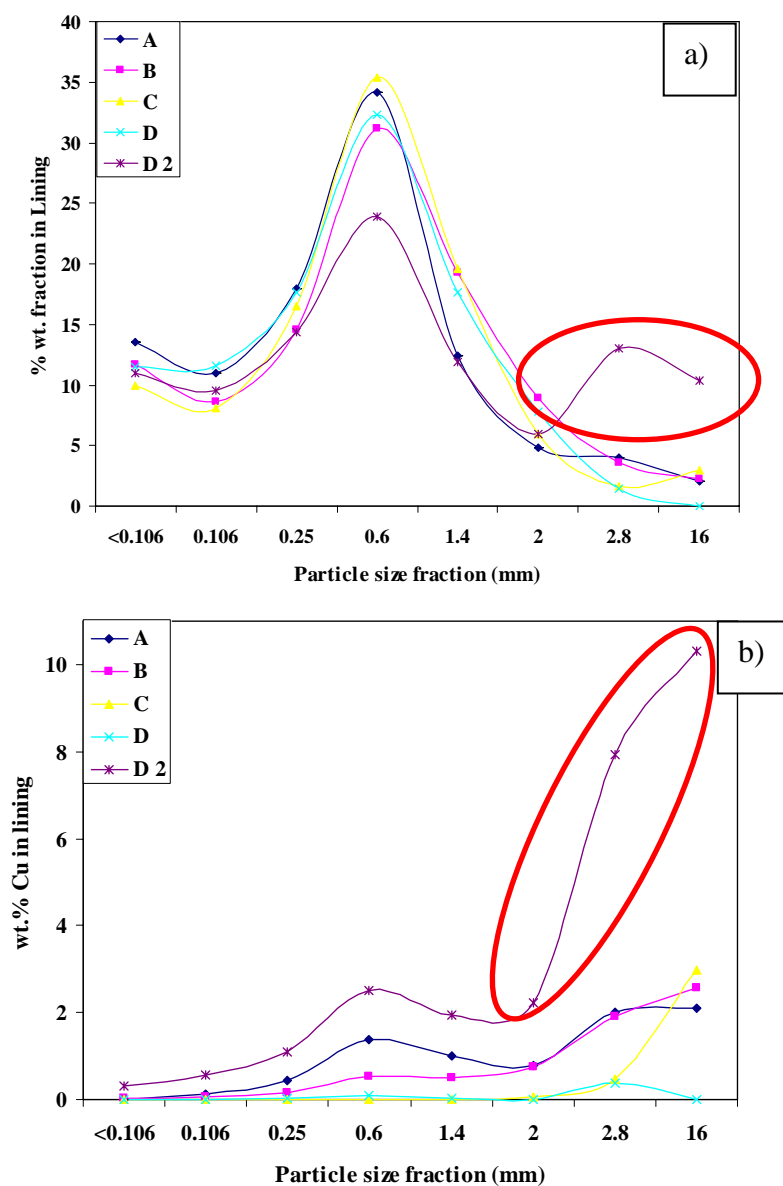


Figure 2.9. a) Particle size distribution of crushed samples (error ~7%) and b) distribution of total copper content at each particle size fraction in crushed lining (error ~8%).

Figure 2.9 summarizes the particle size distribution for each of the crushed samples and Figure 2.9b illustrates the distribution of copper at each size fraction. The material retained at 16mm mesh is the amount of copper that is effectively screened as strips. The three inductor samples from A, B and C have copper content of 2.1%, 2.5% and 3% respectively ( see Figure 2.9b) as expected from the characterization indicating that the inductor linings are potential material to be recycled.

The particle size distribution and copper distribution for type C refractory indicate that 90% of the copper in the spent lining is present as oversize in the 16mm size fraction (see Figure 2.9b). However, for type A and B type refractory, copper is widely distributed in subsequent fine size fractions. Screening of copper (wt. %) at each subsequent fine size fraction depends on the amount of crushed lining attached to the copper particles (see Figure 2.9a). The copper from +2.8mm and +2mm size fractions in type A and B refractory samples can be screened. Therefore, the screening procedure can be modified based on the copper distribution in each size fraction for effective separation.

The type D refractory has lower copper content than the inductors in agreement with the characterization results. However, the new spent lining samples of type D2 show significant metal penetration and was much higher than the inductor linings. The particle size distribution and copper distribution for type D2 refractory indicate that majority of copper is present as oversize in 16mm and 2.8mm size fraction (see Figure 2.9) making it favorable for recycling. For further understanding of the screen procedure, the cumulative copper present in each refractory lining was summarized in Figure 2.10.

For type D refractory in Figure 2.10, the percentage of copper present as oversize in 2.8mm size fraction constitute 85% of the total copper present in the lining samples and changing the screening procedure from 16mm mesh size to 2.8mm would recover 85% of the total copper. Similarly for type A refractory, screening with 2mm mesh opening would recover 60% of copper. As discussed earlier, all the results were reported as total copper content in the spent linings, the total metal content however, is 1.1 times higher than the reported values and precious alloying elements present in brass would add more value to the recycling process.

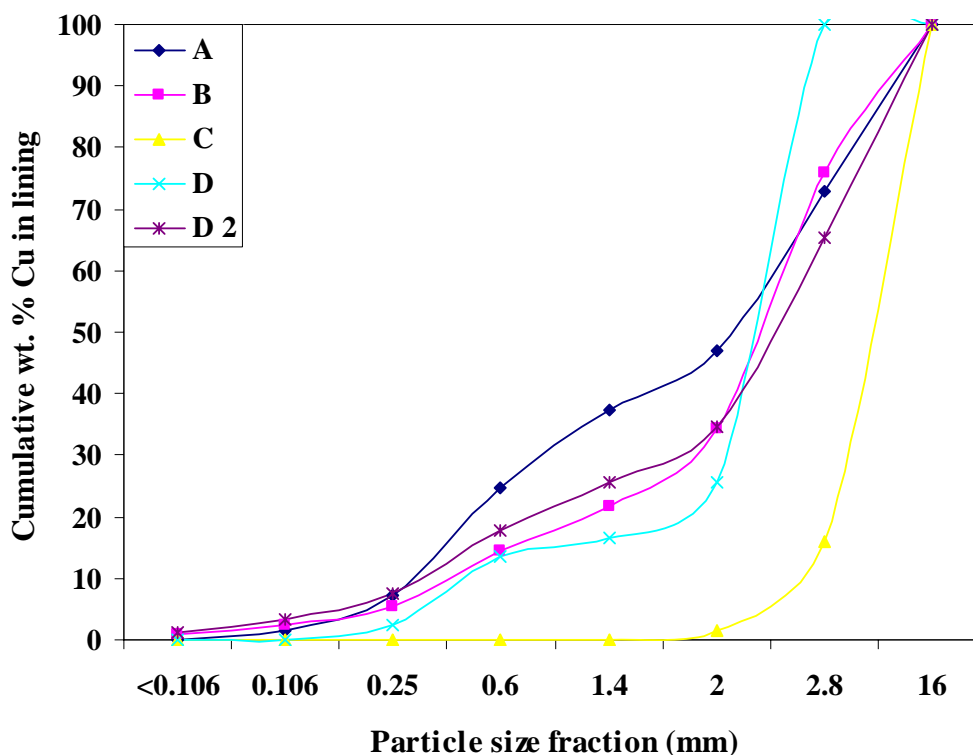


Figure 2.10. Cumulative copper distributions after crushing for all the lining samples at each specified size fraction (error ~10%).

In Figure 2.10, it is observed that there is wide distribution of copper in the type D2 refractory samples at each size fraction. However, ~75% (by weight) of total copper present in the lining sample is present at 2mm size fraction as oversize with ~25% (by weight) of the total crushed lining. Hence, changing the screening procedure using 2mm mesh opening instead of 16mm mesh opening would recover 75% of total copper. The results for recovered copper by screening and copper content by acid leaching for each refractory lining are tabulated in Table 2.5. The Table 2.5 summarizes the recovered copper and copper content obtained by chemical leaching. ~90% of total copper in type C refractory is present as strips which can be recovered by screening. From Table 2.5, the type A and B refractories have ~45% recovered copper in brass strips however, suitable screening procedure could liberate ~60% of copper.

Table 2.5. Copper distributions in the crushed refractory linings.

Type of Refractory	wt.% Copper in Lining		
	Recovered strips (+16mm)	Chemical leached	Total Copper in lining
A	$2.1 \pm 0.5$	$5.8 \pm 1.2$	$7.9 \pm 1.7$
B	$2.5 \pm 2.5$	$4.3 \pm 2.3$	$6.8 \pm 4.8$
C	$3 \pm 0.2$	$0.5 \pm 0.1$	$3.3 \pm 0.3$
D	0	$0.5 \pm 0.4$	$0.5 \pm 0.4$
D2	$10.3 \pm 5.8$	$16.3 \pm 4.7$	$26.6 \pm 10.5$

The test samples representative of all the types of refractory linings landfilled every year have been analyzed for copper content. The separated brass strips were copper rich (85% to 90% Cu) and the average copper content in the test samples were summarized in Figure 2.11. The results for type D refractory had significant variation in the two sets of samples. The two samples were analyzed with X-ray diffraction (see Figure 2.12) to understand the cause for increased metal penetration.

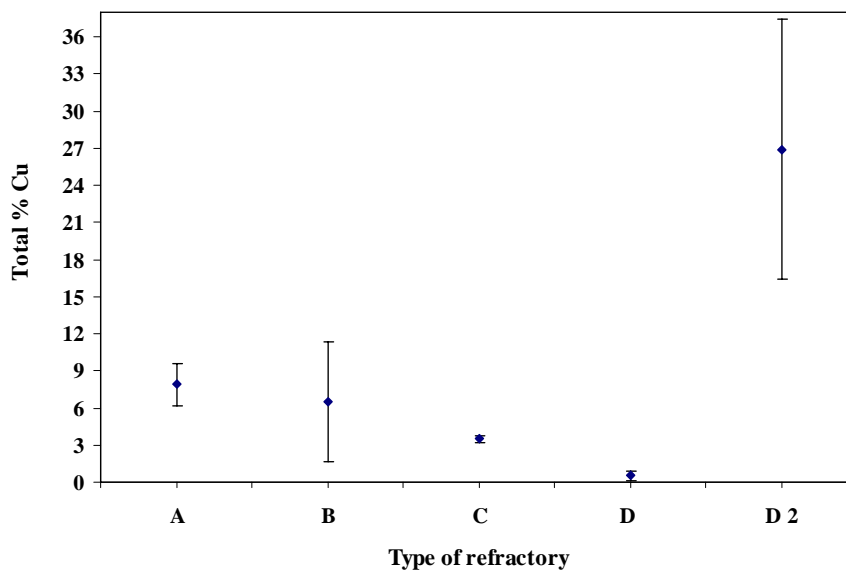


Figure 2.11. Average copper present in test samples of different refractory types.

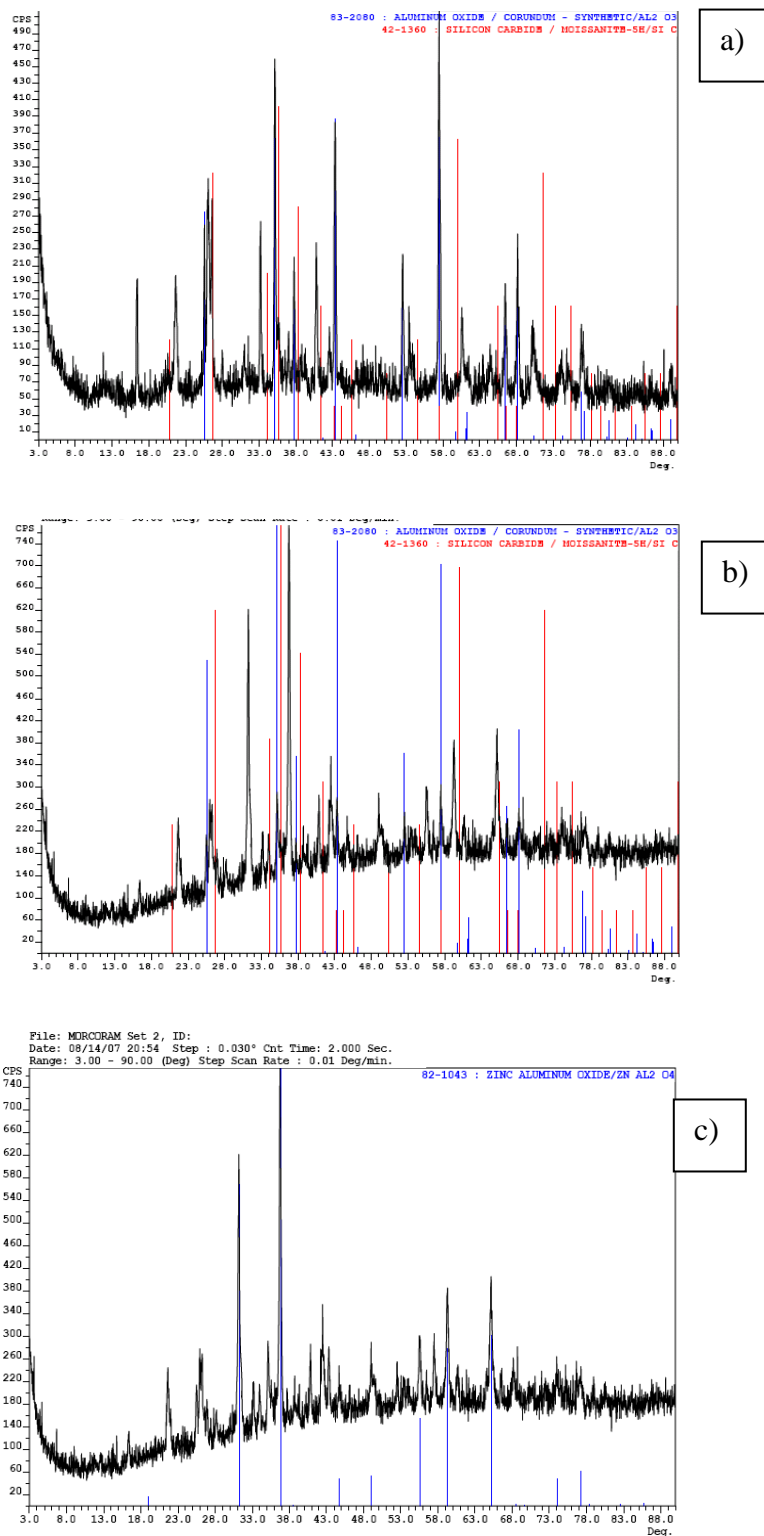


Figure 2.12. XRD patterns generated for samples from a) D type refractory b) D2 type refractory c) D2 type refractory indicating the presence of spinel phase.

In Figure 2.12, spinel phase was identified at ~31 and 37 degrees and this peak was absent in the Figure 2.12a indicating the possibility of wetting of alumina by copper alloy for samples from D2. The alloying additions of Mg and Mn produce spinel type phase at the interface between the copper melt and the refractory layer thereby breaking the matrix of the refractory layer [19-22]. Numerous studies have indicated that alloy additions of titanium, tin, magnesium and manganese have pronounced effect on wetting characteristics of alumina by copper [19-22]. The Cu-Mg/Mn alloys especially have significant effect on the wetting characteristics. The spinel  $MAl_2O_4$  (where M = Mg or Mn) formed would continuously react with  $Al_2O_3$  until equilibrium is attained, considerably damaging the refractory matrix and facilitating increased metal penetration in the refractory lining [22]. Therefore, increased metal penetration in samples from D2 refractory was attributed to the spinel formation.

The copper content analyzed by crushing and grinding followed by chemical leaching indicate that majority of the copper was present as brass strips in the refractory lining and 65% to 95% copper rich product can be effectively recovered. The secondary recovering methods were effective in recovering 100% of copper present in the lining samples but the expenses incurred might exceed the benefits of recycling.

For refractory types A, B, and C used in inductors, the total copper content (wt.%) screened using 16mm mesh was found to be 2.1%, 2.5% and 3% respectively, indicating significant metal penetration. Hence, the inductor linings are potential materials for recycling. However, the refractory type D used for furnaces had varied results but considering the fact that the brass producer has maximum tonnage (five million pounds) of this type of lining landfilled every year, it can be a potential material to be recycled.

### 3. PROCESSING OF NEW REFRACTORY CASTABLES USING SPENT LINING

#### 3.1. BACKGROUND ON CASTABLES

Refractory castables comprise a major group of monolithic refractory and have supplanted shaped refractories in most of the applications because of superior properties and ease of installation. The mix of the castable varies from simple mixes with one binder to complex multi-phase and blends of novel materials to target specified applications. Refractory castables are comprised of aggregate/refractory grains, matrix components, binders and admixtures [23]. Most of the castable blends are either hydraulic or chemical set with water as the most common setting agent. The most common binder is calcium aluminate cement available in various grades depending on the percentage of alumina.

The alumina and alumino-silicate refractory castables are classified based upon the cement content in the castable. Conventional castables ( $> 2.5\%$  CaO), low cement (1.0 - 2.5% CaO), ultralow cement (0.2 – 1% CaO) and no cement ( $< 0.2\%$  CaO) castables form the classification. The admixtures are novel additions to impart special properties to the castable. SiC is sometimes incorporated in the castable blend as an anti-wetting component to facilitate the use of certain melt alloy compositions in the furnace. The preparation of refractory castable includes mixing and blending, drying/curing and firing. The particle size distribution has a major impact on the properties of the castable.

**3.1.1. Particle Size Distribution.** Comminution processes result in a continuous particle size distribution and hence can be used to process new castables. The fine particles fill up the voids between large size particles [24]. A discrete particle size distribution cannot attain maximum density as the volume of the voids to be filled cannot be completely filled by cement and silica fume (typically -90 microns). The void area or porosity of the castable would increase as a function of the decreasing ratio between the largest diameter particles (DL) and the smallest diameter particles (DS).

Highly dense castables are prepared by 'fill out' which essentially implies that certain fillers/modifiers are used to obtain dense packing of particles. Many mathematical models have been developed [25-27] and three major distribution principles for the particle size distribution of the aggregates are proposed which are Andreasen distribution (equation 1.1), Furnas distribution (equation 1.2) and Funk-Dinger model (equation 1.3)



for crowded particulate suspensions. All the three principles define particle size distribution in terms of largest particle diameter against cumulative percent finer than (CPFT).

$$\frac{CFPT}{100\%} = \left( \frac{D}{D_L} \right)^n \quad (1.1)$$

$$\frac{CFPT}{100\%} = \frac{(D)^n - (D_S)^n}{(D_L)^n - (D_S)^n} \quad (1.2)$$

$$\frac{CFPT}{100\%} = \frac{(D)^{\log r} - (D_S)^{\log r}}{(D_L)^{\log r} - (D_S)^{\log r}} \quad (1.3)$$

Where D - diameter of the particle

$D_L$  - diameter of largest particle

$D_S$  - diameter of smallest particle

n - distribution modulus

The Funk-Dinger model is a modified Furnas equation, where the distribution modulus  $n = \log r$ ; r is defined as the ratio between two consecutive sieve opening sizes and is most widely used for a sequence of comminution and sieve analysis operations.

The Andreasen distribution does not define the smallest particle diameter and maximum density is attained by adding smaller particles which fill the void area. However, the Furnas distribution introduces the smallest particle size diameter and calculates the maximum allowable porosity for a defined  $D_S/D_L$  ratio. As the  $D_S/D_L$  ratio decreases, the particle size distribution becomes wider thereby filling all possible voids

and achieving maximum density attainable by particulate materials. The distribution modulus ( $n$ ) was found to be 0.37 [27] for maximum packing, allowing blend suppliers to calculate particle size distribution for specified porosity levels. This is particularly useful in recycling of spent refractory linings, as the crushed lining is subjected to particle size analysis and the particle size distribution is calculated to process a new castable blend incorporating all of the crushed particles.

The rheological factors determining the flow properties of the castable do not conform to the calculated mathematical factors and more often a factor of 0.21 is used in industries. Since the porosity levels increase with this packing factor, industrial particle size distribution generally follows bimodal or multi-modal distributions wherein micron and submicron size additives are added to fill out the pores in the castable, improving the overall performance of the castables.

**3.1.2. Curing and Firing.** The blend or mix of aggregates, binders and admixtures can be either chemically set or hydraulically set. The type of bonding agents used in castables have been increasing and many new types have been developed including non-cement bonds such as hydratable alumina, clay, silica and alumina gels, and chemical bonds such as phosphates and alkali silicates with each binder attributing special properties depending on the application.

The present study uses calcium aluminate cement as the binding agent for a proper blend of spent lining and fresh virgin lining aggregate. The binding mechanism of calcium aluminate has been investigated and reported [22]. The principal hydrating phase is calcium monoaluminate-  $\text{CaO} \cdot \text{Al}_2\text{O}_3$  or CA. CA upon addition of water changes to  $\text{C}_3\text{AH}_6$  which is the stable hydratable phase with curing temperatures above  $35^\circ\text{C}$ . However, lower temperatures are not favorable as CA would form metastable hydrates which upon further heating would convert back to stable  $\text{C}_3\text{AH}_6$ , but the conversion is accompanied by phase volume shrinkage leading to a weak bond.

Dehydration takes place during the curing stage and generally in the temperature range of  $210\text{-}315^\circ\text{C}$ . The curing time is generally long as the smaller size fractions which are used to attain maximum density delay the dehydration process. Finally, after curing the castables are fired to gain significant strength and wear resistance. The firing

temperature is selected as the temperature at which the refractory has maximum modulus of rupture.

**3.1.3. Processing of Castables from Spent Refractory.** The crushed lining material of type C refractory obtained after crushing and screening to remove metal was used for processing of new castables. The particle size distribution of the blend influences the properties and performance of castables. The crushed lining has a continuous particle size distribution but the distribution does not follow the mathematical distribution models discussed in Section 3.1.1. A small crucible mold was designed for castable preparation (see Figure 3.1). The top plunger of the mold was designed to moderately ram the castable mix for achieving better densification.

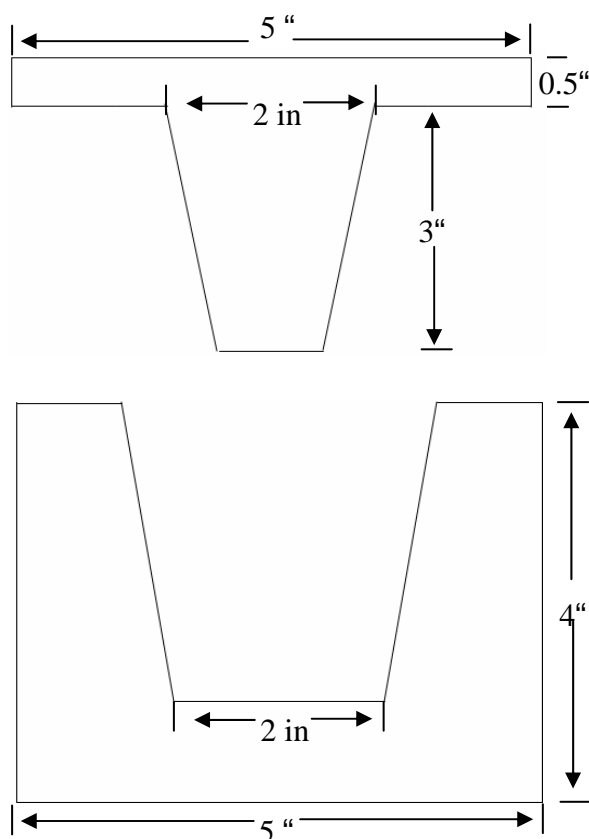


Figure 3.1. Crucible mold design for processing castables from virgin and crushed spent lining.

Virgin refractory castable mix of type C (see Table 2.1 in Section 2.1) was obtained from industry for a base line comparison with crush refractory lining of type C. The material datasheet for the virgin castable mix is provided in Appendix B.

### 3.2. EXPERIMENTAL PROCEDURE

Initial trials were done to understand the particle size distribution of the virgin refractory mix and determine the optimum particle size distribution based on the theoretical model. Sieve analysis of the virgin mix indicated that the castable aggregate distribution was a multi-modal distribution.

The initial trial used the virgin refractory mix with 5-6% water and the castable was found to be porous as shown in Figure 3.2. Porosity was due to the fact that the diameter of largest particle was greater than one-third of the wall thickness. Normalization is the process of screening the undesired large diameter particles and extrapolating the remained particle size distribution such that the distribution modal is not disturbed. After the first trial, the refractory mix was normalized such that the maximum particle diameter was restricted to 2.3mm and with the normalized particle size distribution (see Figure 3.3), a new castable was prepared (see Figure 3.2 b). The tabulated particle size distribution is provided in Table C.1 in Appendix C.

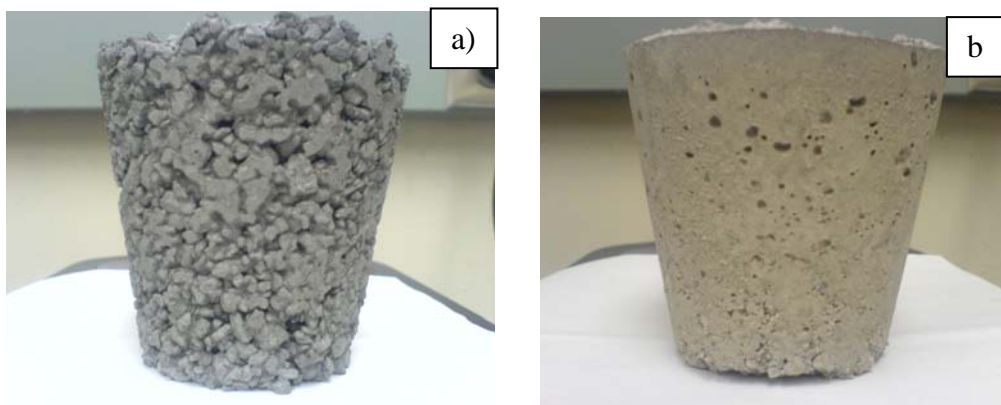


Figure 3.2. a) Porous castable prepared from virgin castable mix b) dense castable prepared from normalized castable mix of type C refractory.

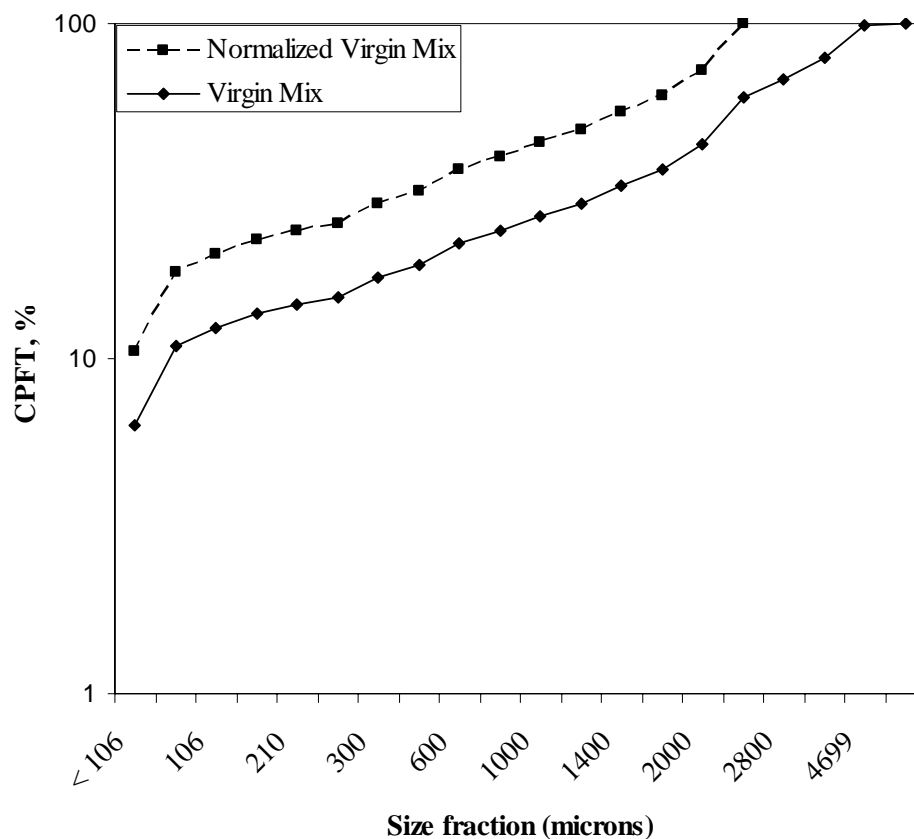


Figure 3.3. Particle size distribution for virgin mix and normalized virgin mix plotted with cumulative percent finer than (CPFT) against size fraction in micrometers.

To compare the performance of castables prepared from crushed spent lining with the virgin lining material, three different blend compositions were analyzed along with virgin refractory for testing their performance. The different blend compositions tested were listed in Table 3.1.

The particle size distribution of the castables followed the normalized virgin mix distribution. The silica fume was added to the crushed lining to achieve increased density. The percentage of silica flour to be added was selected to keep the total silica content of the entire lining to be in the same chemical composition range as prescribed by the refractory material supplier. Secar 51 grade cement was also selected to keep the total alumina content consistent with the prescribed chemical composition of the refractory supplier.

Table 3.1. Blend compositions for different castables.

Castable	wt.% Virgin	wt.% Spent Lining	wt.% cement	wt.% Silica Flour
1	100	0	0	0
2	90	9	0.5	0.5
3	50	45	2.5	2.5
4	0	90	5	5

The experimental procedure was set up for testing the processed castables as described below:

- Determine the particle size distribution of the virgin material.
- Screen the large diameter particles such that the largest particle diameter was 2.3mm and normalize the particle size distribution.
- Add calcium aluminate Secar 51 grade cement (5% maximum) as the binding agent.
- Add silica flour (-90 microns) as described in Table 3.1 to adjust the percentage of fine size fraction and also maintain the chemical composition.
- Cure at 210° C for 12 hours.
- Fire at 1200° C for 6 hours and cool to room temperature.
- Test at 1200° C for 48 hours by adding a mixture of 75% copper and 25% carbon to fill 75% of volume of the crucible (carbon to avoid oxidation of copper).

### 3.3. RESULTS AND DISCUSSION

Figure 3.4 illustrates the castables before firing, after firing at 1200 °C and after testing for 48 hours at 1200 °C.

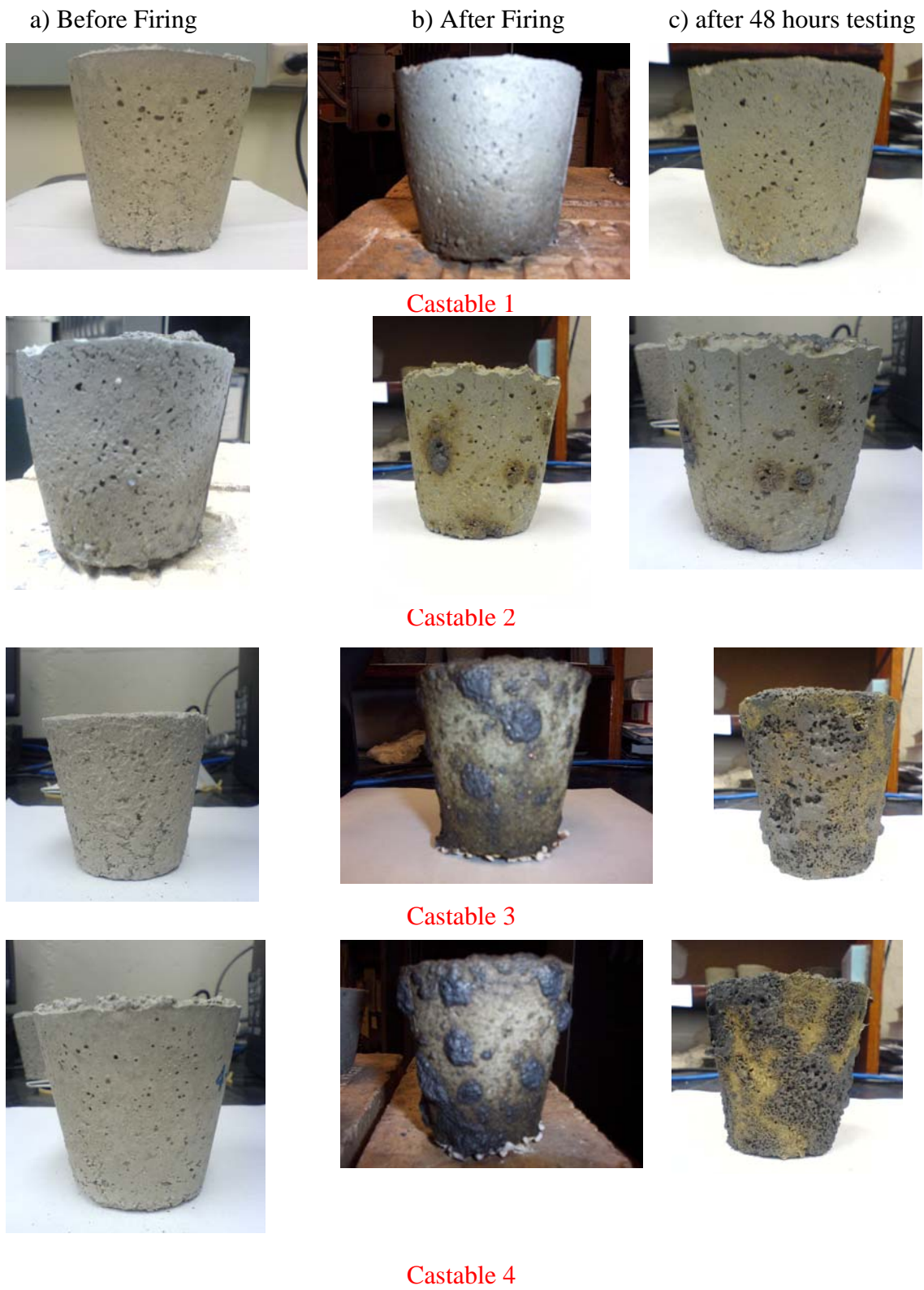


Figure 3.4. Macro photographs of all four castables a) before firing b) after firing c) after testing for 48 hours.

The castable crucibles were fired at 1200 °C and then filled with 75% copper and 25% carbon powder to test the ability of each blend to prevent copper penetration and survive for 48 hours at 1200 °C. The firing cycle was designed based on the ASTM C 401 standard for regular castables.

The macro photographs of the castables 3 and 4 (see Figure 3.4) after firing at 1200 °C for 6 hours have significant surface growth because of scab formation. The scabs are formed due to the oxidation of copper present in the brass particles of crushed spent lining. However, there was no scab formation in castable 2 which has 9% of the crushed spent lining indicating the possibility of using the castable 2 for low duty applications.

The macro photographs of the four castable crucibles after testing for 48 hours (see Figure 3.4) have no noticeable change with regard to copper oxidation in the lining, indicating that the entire copper present in the crushed lining was completely oxidized during the firing stage. However, there is noticeable discoloration in castables 3 and 4 indicating the possibility of copper penetration.

Cross-sectional samples were taken from the bottom of the castable crucibles (see Figure 3.5) and analyzed using stereoscope for possible metal penetration (see Figure 3.6).

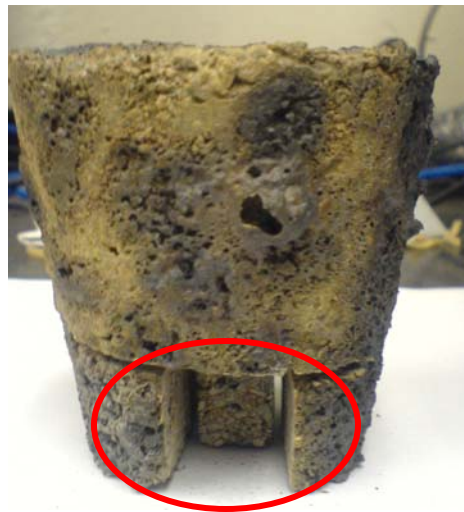


Figure 3.5. Macro photograph of castable 4 indicating the location of all cross-section samples.



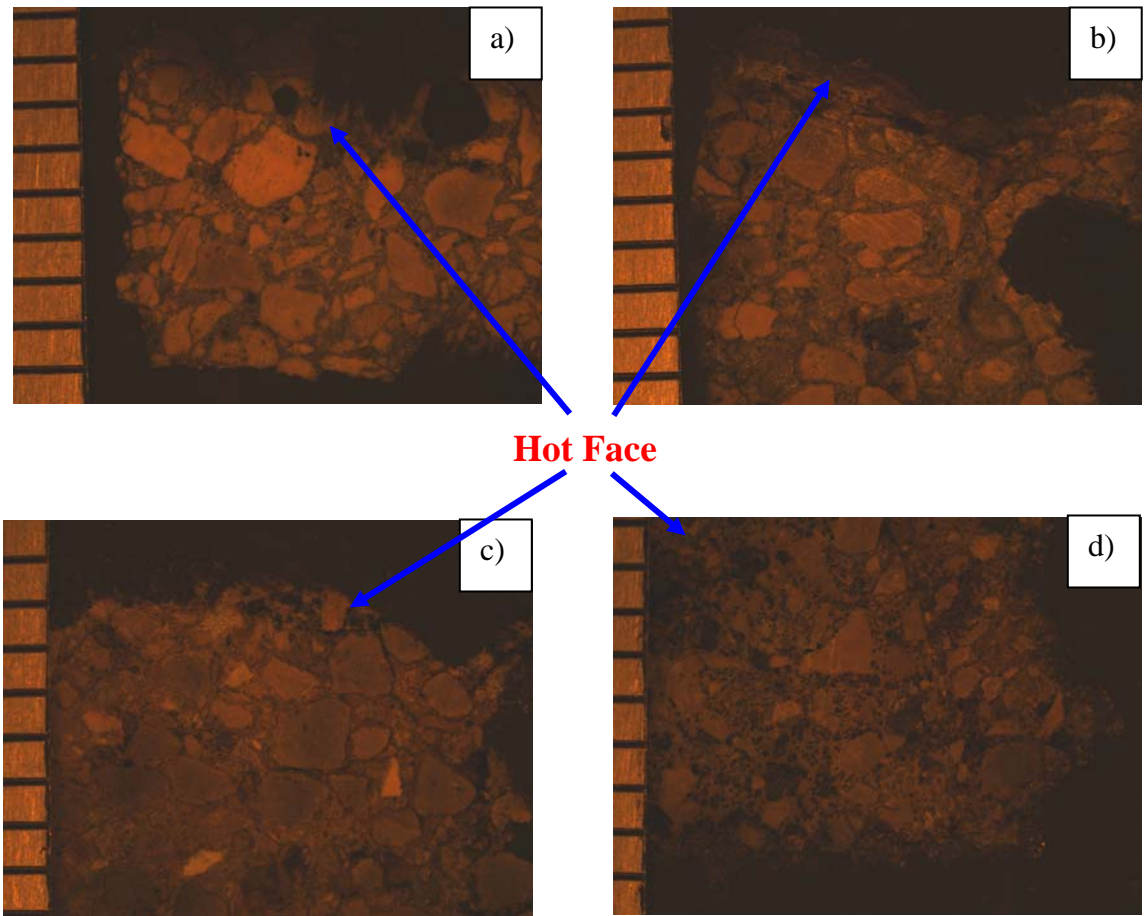


Figure 3.6. Stereoscope cross-section images from hot face to cold face of a) castable 1 – virgin blend b) castable 2 - '90-10' blend c) castable 3 – '50-50' blend and d) castable 4 – blend of crushed spent lining.

Figure 3.6 illustrates the cross-section images from hot face to the cold face. Copper penetration could not be observed from the stereoscope images for the four castables. Hence, the cross-section samples were analyzed for the hot face using optical microscopy (see Figure 3.7).

The walls of the crucibles have also been analyzed along with the cross-sectional samples. The cross-section of the wall of the crucibles did not yield significant results with respect to the metal penetration and hence the cross-section samples were analyzed for metal penetration.

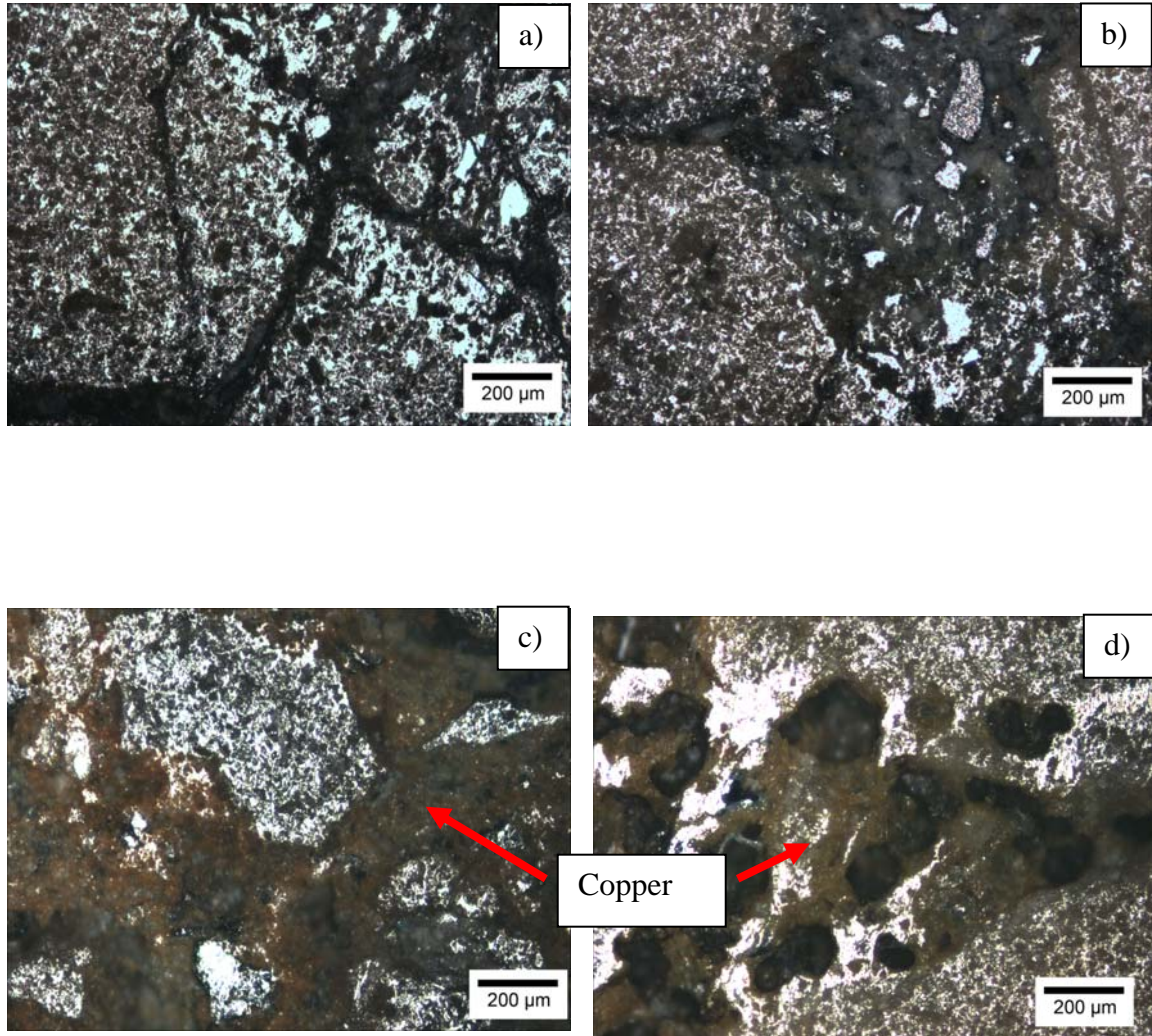


Figure 3.7. Optical micrographs of hot face of four types of castables showing no metal penetration after 48 hours of testing a) Castable 1, b) Castable 2, c) Castable 3, d) Castable 4.

No metal penetration was found for castable 1 and 2. The macro-photos also showed no copper oxidation after firing for castable 2 (90% virgin-10% crushed lining). Therefore, the mix 2 can be used as a back up layer in the melting furnaces. However, copper penetration of ~11% of the cross-section thickness for castable 3 and ~13% for castable 4 was observed. Hence, for further studies, the crushed lining can be pre-fired to oxidize the copper or can be chemically leached to remove the copper, and then use the spent lining for preparing castables.

## 4. INDUSTRIAL PROCESS DESIGN AND SCALE UP

### 4.1. PROCESS DESIGN

An industrial scale up model was developed to summarize the economic costs and benefits of refractory recycling and provide a method for achieving optimum benefits. The present section discusses the method of developing the economic model to design and scale up the process to industrial operations using METSIM version 15.12 software.

The METSIM software provides models to analyze different comminution techniques, the power draw for each process, and gives comprehensive data on the particle size distribution obtained from each operation. The software has to be backed by preliminary data to design a comminution flow chart. The Bond Work Index ( $W_i$ ) and dimensions of the process equipment are important parameters for designing the flow chart. Bond [28, 29] defined work index as a comminution parameter used to calculate the energy consumed or expended in grinding the feedstock to 80% passing of specified product particle size. The Bond Work Index test is used to evaluate the grindability of feedstock based on the Bond's [29] third theory of comminution given in equation 4.1

$$W = \frac{10W_i}{\sqrt{P}} - \frac{10W_i}{\sqrt{F}} \quad 4.1$$

Where  $W$  - work input in kWh/short ton,

$W_i$  - work index calculated by Bond Work Index test

$P$  - 80% passing product particle size and

$F$  - 80% passing feed particle size

**4.1.1. Bond Work Index Test Procedure.** The test is a measure of the grindability of the feedstock. A short description of the standard test procedure [30]:

- Crush dry feed to 100% passing 3.3mm mesh.
- Calculate packed density and 700ml constant feed for ball mill bond work index test.
- Sample using splitting techniques to obtain a representative feed from the crushed lining.
- Sieve analysis of the feed to understand the particle size distribution and calculate 80% passing feed particle size.
- Run the mill for 50 revolutions and re-circulate the over-size feed to the mill thereby maintaining constant volume of 700ml.
- Repeat the test process until steady state is attained for atleast the last two periods. Steady state is obtained for 250% recirculating load.
- Calculate the net product produced per mill revolution of grindability of product (Gpr).
- Sieve product and 80% passing product particle size is calculated.

The work index is calculated using Bond's formula for Work Index given in equation 4.2

$$W_i = \frac{44.5}{P_1^{0.23} G_{bp}^{0.82} \left[ \frac{10}{P^{0.5}} - \frac{10}{F^{0.5}} \right]} \quad (4.2)$$

Where  $P_1$  – micron size at which grindability test was conducted,

$G_{bp}$  – Grindability value,

P -80% passing product size in microns and

F- 80% passing feed size in microns

**4.1.2. METSIM Design.** METSIM software was used to evaluate the power draw for the comminution operation and optimize the design for using various crushing and grinding equipment. The software calculates particle size distribution for the type of crushing and grinding equipment based on the input parameters such as open side setting, closed side setting and throw of crushing equipment and mill diameter, critical mill speed for ball mill equipment. The METSIM help files for the equipment used in the design and required parameters for the working of the design are briefly described in Appendix D. The particle size distributions obtained from the model were used to calculate the particle size distribution for processing new refractory castables.

## 4.2. BOND WORK INDEX TEST RESULTS

A sample splitting technique was used to select a representative feed sample and to test the grindability of the spent lining. The initial feed stock of type A refractory was crushed to less than 3.3mm and taken as feed for analysis. The as-received type A refractory lining sample used in the inductors was taken as a representative sample for the six types of refractory as the chemical composition for inductor linings was similar. The packed density of the crushed spent lining feed was calculated to estimate 700ml volume of material for analysis. Particle size analysis of the feed was done by vibratable sieve shaker to calculate the 80% passing feed particle size. The product size was selected based on the minimum copper globule size estimated from the SEM image of the feed material. The 80% passing product size was taken as 106  $\mu\text{m}$  which was the minimum copper globule size as measured from SEM. The Bond Work Index test was performed sequentially on the crushed lining without screening out the copper. The preliminary calculations are:

- Lab Mill Feed =  $1.709 \text{ g/cm}^3$  equivalent to 1196.3g (700cc) in mill.
- Ideal Potential Product = 341.8 g.
- Average of last 2 periods = 247% circulating load.
- Grindability at 106 microns = 0.745 net grams per revolution.

The test reached steady state in fifth, sixth and seven periods. The graph between the net grams per revolution against number of period was plotted as shown in Figure 4.1.

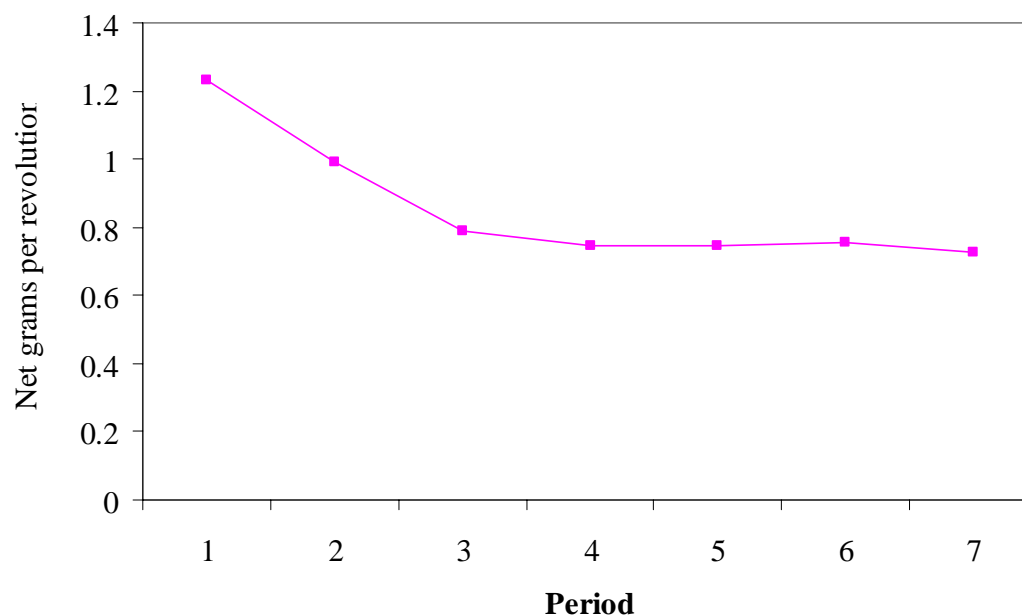


Figure 4.1. The net grams per revolution plotted against period number showing steady state for fifth, sixth and seventh period.

The results for the Bond work index are tabulated in Table 4.1. The feed, product and circulating load size distribution were illustrated in Figure 4.2. The bond work index  $W_i$  was calculated from equation 4.2 and was found to be 21.2 kWh/st.

Table 4.1. The BWI test results for crushed lining

Period	Revolutions of Mill	Grams of Product	Grams in Feed	Net grams Produced	Net grams per revolution
1	70	164.4	78.2	86.20	1.23
2	269	278.0	11.0	267.0	0.99
3	327	275.2	18.3	256.9	0.78
4	410	323.0	18.0	305.0	0.75
5	432	343.9	21.4	322.5	0.74
6	427	345.7	22.5	323.2	0.75

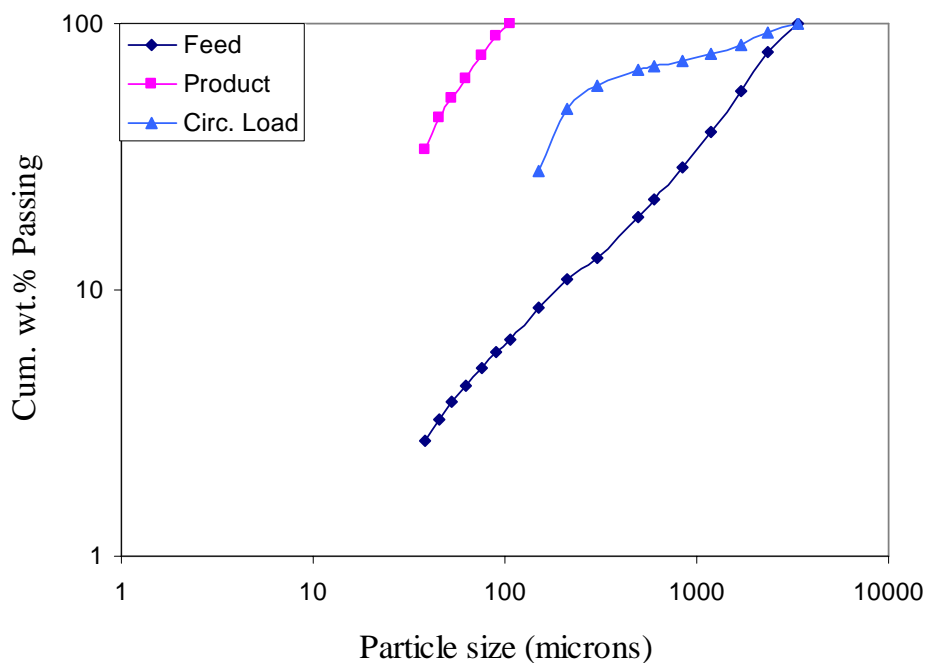


Figure 4.2. The particle size distribution of feed, circulating load and product

The particle size distribution determines the amount of power drawn by the ball mill. An increase in the 80% passing product decreases the power draw of the process as it requires less grinding action.

### 4.3. METSIM PROCESS DESIGN

The comminution operations are energy intensive and therefore the energy requirements might inhibit recycling benefits. The energy expended for liberation of copper from the spent lining was considered as a crucial parameter. The other important economic parameters are the cost of liberated copper and the cost to landfill. The cost of landfill for specific refractory type is constant; however, the cost of copper is variable thereby the economics of the recycling process can be evaluated depending on energy consumption and copper scrap cost for the present model. To relate energy consumption

to cost benefits, the Bond work index was used to design the energy requirements for crushing and grinding of the large refractory pieces to smaller fractions.

The METSIM model was an attempt to optimize the energy consumption for maximum copper yield from lining material with minimal energy and to also obtain particle size distribution which can be used to prepare and process new refractory castables. The preliminary model was used to compare the energy expended to crush the feed into the required product 80% passing size and also a particle size analysis for the two primary crushers - jaw crusher and cone crusher. Preliminary studies were done by modeling flow charts using a jaw crusher (CRJ) and roll crusher (CRR) and ball mill (MLB) and screen (SCK) in sequence. The flow sheet for “jaw crusher and ball mill” operation is illustrated in Figure 4.3. The “cone crusher and ball mill” model was designed similar to the Figure 4.3 except for the replacement of jaw crusher and roll crusher with a cone crusher. The mass flow rate for all the models was taken as 10 metric ton/ hr. The sequence of operations is connected with lines which are called streams.

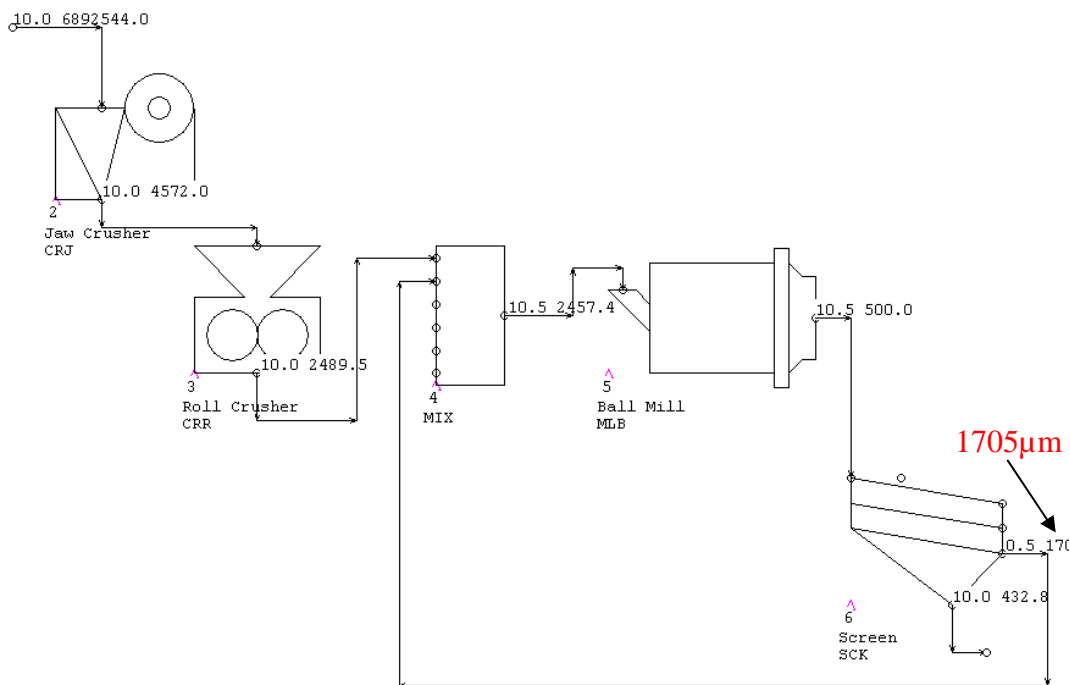


Figure 4.3 METSIM grinding circuit (Jaw crusher model) for calculation of comminution energy for refractory lining showing mass flow rate and P80 for respective streams



In Figure 4.3, there are numbers along the exit of each stream. The numbers represent the mass flow rate 10 tons/hr and P80 of the mass passing through the stream. The oversize material after screening has higher P80 (1705  $\mu\text{m}$ ) because the coarse particles from the ball mill and roll mill are screened and constitute much lower percentage of the entire material. The jaw crusher model has input parameters of 160mm open side setting and 155mm throw. The dry grinding factor for the circuit was taken as 1.3 as defined by the METSIM software and energy expended to crush the feed was calculated for 106  $\mu\text{m}$ , 250  $\mu\text{m}$ , 500  $\mu\text{m}$ , 750  $\mu\text{m}$  and 1000  $\mu\text{m}$  product 80% passing particle sizes. The parameters for ball mill are driven by industrial specifications [33]. The details of crusher and ball mill and the model results were tabulated in Table 4.2.

Table 4.2 Power Draw and Dimensions for the Process Design and Scale up model

P <sub>80</sub> ( $\mu\text{m}$ )	Crusher Power Draw (kW)	Ball Mill Diameter (m)	Ball Mill Length (m)	Ball Mill Power Draw (kW)
Jaw CR+Ball Mill				
1000	27.925	2.00	1.10	53.898
750	27.925	2.12	1.17	67.070
500	27.925	2.37	1.15	90.175
250	27.925	2.37	1.88	147.269
106	27.925	2.75	2.15	253.629
Cone CR+Ball Mill				
1000	23.432	2.00	1.55	96.890
750	23.432	2.12	1.52	111.01
500	23.432	2.37	1.38	136.715
250	23.432	2.37	2.10	207.55
106	23.432	2.75	2.27	334.068
DS Jaw CR				
400	15.780	na	na	na
624	17.110	na	na	na
680	17.780	na	na	na
780	19.670	na	na	na
870	31.050	na	na	na

na – not available

To compare the power draw and particle size distribution between a jaw crusher and cone crusher, a similar model was created for a cone crusher. The power draws for screening and mechanical separation were minimal with respect to the power draw of the comminution operation and hence were neglected for energy calculations.

A third model was developed with a double stage jaw crusher excluding the ball mill and roll crusher. The flow chart for the double stage jaw crusher model is illustrated in Figure 4.4.

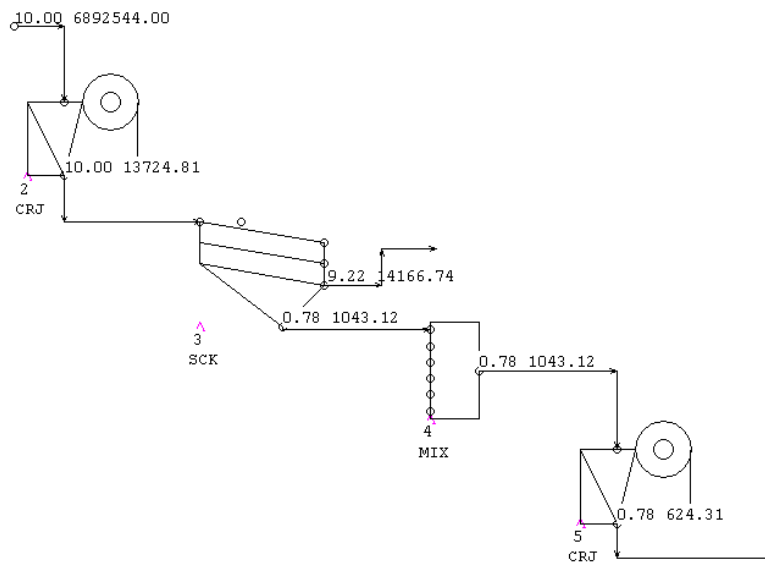


Figure 4.4. Process flow chart developed in METSIM for double stage jaw crusher

The double stage jaw crusher (CRJ) would eliminate the use of ball mill. Since, the ball mill is energy intensive as found from Table 4.2; the double stage jaw crusher would result in significant economic benefits. A double stage jaw crushing operation with

screens (SCK) in between the two crushing operations would allow control over the particle size distribution.

#### **4.4. RESULTS AND DISCUSSION**

The jaw crusher and gyratory crusher are primary crushing equipment with the ability to handle large chunks of material, in comparison to the cone crusher which is a secondary crusher with a relatively smaller opening size and cannot handle large chunks as compared with the primary crushers. Hence, the energy consumption for the cone crusher model was higher when compared with the energy consumption for a jaw crusher. Also, the jaw crusher is economical when the feed rate is less than 187.5 tons per hr [32]. For further optimization of the energy consumption; the characteristics and importance of the ball mill were considered.

The ball mill is a grinding mill for reducing the size of the coarse feed from crushers to finer micron size product material and has maximum energy utilization in the model. For the present application, the fraction of fine particles was not required for metal liberation; however the finer size fraction is critical for processing new refractory castables. Also the ball mill is an expensive capital investment for processing material with a low feed rate. Hence, a double stage jaw crusher model was developed in METSIM and the power draw was calculated (see Figure 4.4).

The double stage jaw crusher model was restricted by P80 (product 80% passing) particle size from 870  $\mu\text{m}$  to 400  $\mu\text{m}$ . The energy consumption from all three models is summarized in Figure 4.5.

The particle size distribution from a double stage (DS) jaw crusher model was compared to the theoretical particle size distribution used in Chapter 3 Section 3.1 are illustrated in Figure 4.6. Theoretical particle size distribution and the particle size distribution obtained through METSIM models are different in comparison with the industrial distribution and therefore, fines are incorporated to fit the industrial particle size distribution.

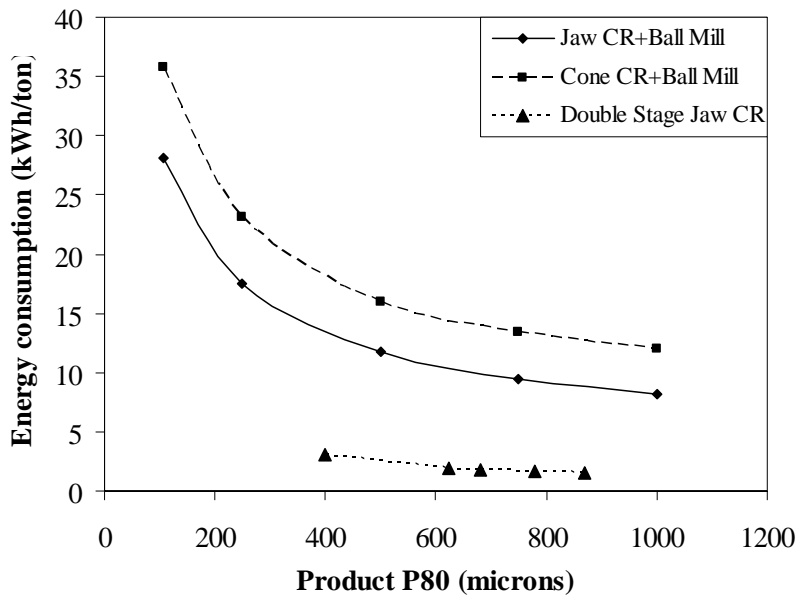


Figure 4.5 Comparison of three models based on the energy expended to crush to a specified product 80% passing

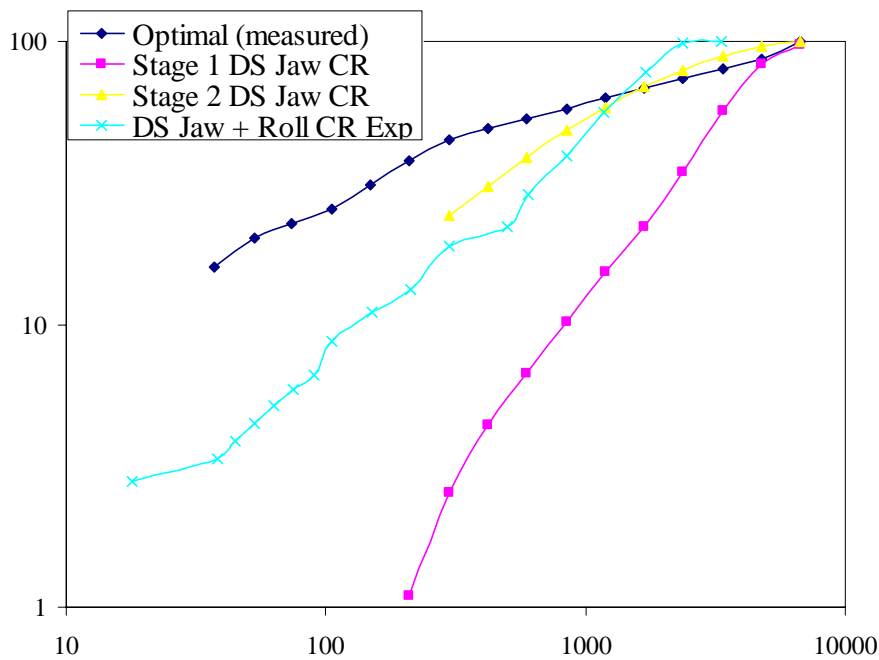


Figure 4.6 Particle size distributions obtained from double stage (DS) jaw crusher model compared with optimal distribution

In the Figure 4.6, the percentage of fines generated in a double stage jaw crusher as per the METSIM model was found to be much higher than the other models developed. The 'DS Jaw + Roll CR Exp' was the particle size distribution obtained experimentally which does not comply with the theoretically developed model. Therefore, fines have to be added to the product obtained by crushing and grinding to build a multi-modal distribution suitable for preparing new castables. The industrial multi-modal distribution is quite complex [34] and cannot be match fit with the simple theoretical models developed. Hence, based on the industrial design, fines have to be incorporated to achieve good castable properties.

However, a double stage jaw crusher utilizes lower energy than other comminution operations. Hence, it is recommended that double stage jaw crusher liberates the entrapped metal and the crushed lining that is obtained can be added to a fine distribution mix to prepare new castables. The total cost benefits to recycle all the materials from the spent refractory lining were evaluated.

The economics of the model results were evaluated using a cost analysis function. The constants used in the value analysis were the cost of brass scrap - \$0.88/lb (25 % of value of copper), cost of landfill - \$18/ton, cost of cement - \$0.31/lb, cost of fresh refractory mix - 0.51\$/lb and cost of electricity - \$ 0.12/kWh. The net value was calculated assuming that 3% of secondary brass can be liberated from the spent refractory lining.

The costs involved for the entire recycling program are estimated as defined by the net value cost analysis function.

$$\begin{aligned} \text{Net value, \$/ton} = & + (\text{Cost of landfill per metric ton, \$/ton}) \\ & + (\text{Metal recovered, mt/hr}) * (\text{Scrap price, \$/mt}) - (\text{Energy consumed,} \\ & \text{kW/hr}) * (\text{Electricity cost, \$/kWh}) - (\text{cost of raw materials, \$/ton}) = \$34.5 / \text{ton} \end{aligned}$$

The cost benefits of recovering all materials and recovering only brass from spent furnace linings are tabulated in Table 4.3. The cost benefits of recovering only brass are higher than recovering all materials. The difference can be attributed to the higher prices of brass which adds value to recovery of only brass and higher prices of cement which decrease the value of recovering all of the materials from spent linings.

Table 4.3. Cost savings for different recycling alternatives

Parameter	Economic Benefits (\$/ ton)
Landfill all materials	-18
Recovery of all materials	+34.5
Recovery of only brass	+40.2

## 5. CONCLUSIONS

The six types of refractory lining samples have been macro-characterized and micro-characterized for preliminary understanding of the samples. SEM/EDS characterization was used to analyze the shape, size and form of brass in the spent lining samples. Based on the SEM/EDS results, copper was physically wetting the lining as there was no reaction at the interface between copper and the refractory matrix.

Brass morphology was determined to be of three different types-strips, globules and wetted layer as thin foils on the ceramic matrix. The formation of strips facilitates liberation of metal from the ceramic matrix by simple crushing and grinding operation. Copper content in the samples was determined by acid leaching followed by quantification with X-ray fluorescence.

The brass strips were separated after crushing operation by screening. The separated strips rich in copper (~90%) can be directly remelted. Two stage crushing and grinding operation liberates 65% to 90% of copper in lining samples. Variation of metallic content in lining samples can be attributed to the alloy chemistry. Alloying elements that have higher wetting angles with alumina create cracks in the refractory lining facilitating increased metal penetration.

The crushed lining was blended with the virgin refractory mix obtained from refractory industry and new refractory castables have been processed. The 50% virgin – 50% crushed lining blend can be used as refractory mortar mix, while the 90% virgin – 10% crushed lining blend can be used for back up lining in furnaces and for lining low duty application furnaces.

The Bond work index test was used to calculate the energy requirements for comminution of the spent lining samples. The lining samples are hard due to the presence of ductile brass in brittle ceramic matrix thereby increasing the power drawn by the comminution operations. Finally, process design model was developed in METSIM analysis software to summarize the cost savings by recycling the spent refractory linings. The Bond work index was used as input parameter for developing value-based model for industrial scale up and thereby evaluating the underlying cost benefits of recycling the spent furnace linings. A value-based model was developed to understand the economics

of recovering only brass and recovering all materials. Although, the economic benefit of recovering only brass is higher, the value of new castables processed from the spent lining can add significant value to recovering all materials.



## 6. FUTURE WORK

Sorting the A, B and C samples which constitute ~13% of the total annual percentage of refractory landfilled, would effectively recover ~70% of the total metallic content entrapped in all of the spent refractory linings. Samples from type D refractory can also be sorted based on visual inspection. The sorting procedure with visual inspection can effectively recover ~90% of the entrapped metal.

The crushed spent linings can be pre-fired to convert copper to copper oxide and the entire mix can be fired to stabilize copper as copper oxide or form copper based spinels (with copper forming solid solution with the spinel). The spinels have higher working temperatures and can be explored as potential applications for recycling the crushed product.

Based on the METSIM models, a cone crusher with adjustable open side setting or jaw crusher with roll crusher are to be studied in detail for economical capital investment. Crushing the spent furnace linings to crushed product with intermediate screening steps can maximize metallic yield.

APPENDIX A

TABULATED RESULTS OF TOTAL COPPER FOR EACH LINING TYPE

Table A1. Summary of results for total Copper present in 'A' type refractory

Sieve size	Size in Microns	Test-1		Test-2	
		Weight Retained (in g)	Total copper (in g)	Weight Retained (in g)	Total copper (in g)
Copper Strips		90.90	86.35	109.0	103.55
7	2800	210.30	127.41	176.1	68.99
10	2000	244.10	61.27	221.3	18.36
14	1400	609.50	67.87	585.6	31.80
28	589	1821.8	97.93	1489.2	38.95
60	250	1005.0	30.70	750.6	13.83
140	106	628.70	07.95	448.5	04.18
Pan	-106	764.00	00.00	560.3	0.00
Product 3		5283.4	393.13	4231.6	176.11
Total		5374.3	479.48	4340.6	279.66
Total Cu in lining, %					
liberated strips			1.60		2.39
leached			7.45		4.16
Total			9.05		6.55
Average				<b>7.9</b>	

Table A2. Summary of results for total Copper present in 'B' type refractory

Sieve size	Size in Microns	Test-1		Test-2	
		Weight Retained (in g)	Total copper (in g)	Weight Retained (in g)	Total copper (in g)
Copper Strips		00.00	00.00	58.44	55.51
7	2800	92.40	40.08	50.4	25.77
10	2000	280.3	9.70	99.7	12.68
14	1400	550.4	3.75	244.3	9.48
28	589	886.9	6.88	396.8	9.05
60	250	413.3	2.64	184.5	2.34
140	106	243.3	1.99	109.8	0.32
Pan	-106	304.5	1.04	162	00.00
Product 3		2771.1	66.11	1085.5	59.68
Total		2771.1	66.11	1143.94	115.20
Total Cu in lining, %					
liberated strips			0		5.1
leached			2.4		5.5
Total			2.4		10.6
Average				<b>6.5</b>	

Table A3. Summary of results for total Copper present in 'C' type refractory

Sieve size	Size in Microns	Test-1		Test-2	
		Weight Retained (in g)	Total copper (in g)	Weight Retained (in g)	Total copper (in g)
Copper Strips		103.0	97.85	53.40	50.73
7	2800	63.28	11.49	25.74	11.47
10	2000	210.18	00.00	103.0	2.05
14	1400	640.46	00.00	379.66	00.00
28	589	1079.1	00.00	736.4	00.00
60	250	466.77	00.00	366.3	00.00
140	106	229.86	00.00	179.4	00.00
Pan	-106	283.13	00.00	219.1	00.00
Product 3		2972.78	11.49	2009.6	13.5
Total		3075.78	109.3	2063	64.2
Total Cu in lining, %					
liberated strips			3.18		2.46
leached			0.38		0.67
Total			3.5		3.1
Average				<b>3.3</b>	

Table A4. Summary of results for total Copper present in 'D' type refractory set 1

Sieve size	Size in Microns	Test-1		Test-2	
		Weight Retained (in g)	Total copper (in g)	Weight Retained (in g)	Total copper (in g)
Copper Strips		00.00	00.00	00.00	0.00
7	2800	39.10	9.32	06.66	3.09
10	2000	217.7	00.00	28.40	0.00
14	1400	325.8	0.87	264.6	0.00
28	589	434.9	3.07	679.0	0.00
60	250	216.9	0.69	395.8	0.00
140	106	141.2	00.00	261.2	0.00
Pan	-106	163.4	00.00	230.5	0.00
Product 3		1539	13.97	1866.16	3.09
Total		1539	13.97	1866.16	3.09
Total Cu in lining, %					
liberated strips			0		0
leached			0.9		0.16
Total			0.9		0.16
Average				<b>0.5</b>	

Table A5. Summary of results for total Copper present in 'D' type refractory set 2

Sieve size	Size in Microns	Test-1		Test-2	
		Weight Retained (in g)	Total copper (in g)	Weight Retained (in g)	Total copper (in g)
Copper Strips		315.2	299.44	308.8	293.36
7	2800	626.2	355.75	319.7	165.2
10	2000	389.6	116.5	115	42.25
14	1400	879.2	107.02	196.1	34.9
28	589	1741.6	132.5	399.4	47.02
60	250	1013.7	49.9	251.6	22.5
140	106	637.3	24.77	176.9	12.05
Pan	-106	732.7	11.35	205.6	7.44
Product 3		6020.3	797.79	1664.3	331.36
Total		6335.5	1097.23	1973.1	624.72
Total Cu in lining, %					
liberated strips			4.73		14.87
leached			13.25		19.9
Total			17.98		34.77
Average				<b>26.6</b>	

## APPENDIX B

### MATERIAL DATASHEET FOR TYPE C VIRGIN REFRACTORY



The type C refractory is a high purity, bauxite base, low moisture, low cement castables used for lining the channel inductor furnaces melting copper based alloys. The castable combines its high alumina base with SiC to provide high strength and low porosity. 5 % to 5.5% is the typical water content for type C refractory castables. The chemical analysis is:

$\text{Al}_2\text{O}_3$  – 73.8% to 78.8%

$\text{SiO}_2$  – 6.35% to 7.85%

SiC – 9.6% to 13.6%

$\text{TiO}_2$  – 1.85 % to 2.35%

The cold crushing strength of  $13.3 \text{ N/mm}^2$  is highest at  $\sim 1200 \text{ }^\circ\text{C}$  and decreases at higher temperatures.

## APPENDIX C

### PARTICLE SIZE DISTRIBUTION FOR PROCESSING NEW CASTABLES

Table A6. Particle size distribution for original virgin blend and normalized distribution for processing new Castables

Particle Size (microns)	Virgin distribution (%)	Normalized distribution (%)
-90	6.3	10.5
90	4.5	7.5
106	1.5	2.4
150	1.2	2.0
210	0.95	1.5
250	0.6	1.1
300	2.2	3.7
425	1.7	2.8
600	3.0	5.0
840	2.0	3.3
1000	2.5	4.3
1180	2.2	3.7
1400	4.06	6.7
1700	3.9	6.5
2000	6.7	11.18
2360	16.5	27.5
2800	7.9	
3350	10.5	
4699	20.0	
6680	1.3	
	100.0	100.0

## APPENDIX D

### METSIM HELP FILES

## D.1 METSIM HELP FILES

METSIM software is developed to design and analyze industrial extraction processes for metal liberation. METSIM v. 15.12 allows designing process flow chart for comparing the power draw capabilities of commonly used industrial comminution equipment and optimize the industrial design and subsequent scale-up. It calculates power draw and also provides comprehensive particle size analysis for each type of equipment but requires preliminary data on the type of material to be used, the Bond Work Index, the initial particle size, flow rate based on different possible model calculation options. The present section lists the principle of operation of cone and jaw crushers and ball mill, the model calculation options, the power draw equation and finally the results of the process design.

**D.1.1. Crusher (Cone-CRC, Jaw-CRJ).** This module does not size equipment; it estimates crusher product particle size distribution.

The CRC unit module is based upon equations derived from regression analyses of screen analysis data of crusher tests performed by the USBM and used by various crusher manufactures. This data is reasonably accurate for normal hard rock of a massive nature but may not apply to salty material.

The module may be used with parameterization calculation option if plant data are available. The parameterization routine uses the algorithms and methodology developed by CANMET (Canadian Center for Mineral and Energy Technology). Once parameterization has been completed or if the CANMET constants are already known then the CANMET option may be used without running parameterization.

Input data is entered via the Parameters input data screen:

*CS - Closed side setting:* The distance between the cone and the side of the crusher when the cone is as close to the sidewall, this measurement is taken at the choke or discharge point. This is a required parameter. The cone crusher uses the closed side setting in its calculations.

*TH - Throw:* The distance the cone can move away from the sidewall. This is a required parameter.

*OS - Open side setting:* The distance between the cone and sidewall of the crusher when the cone is furthest away from the wall taken at the choke point. The open side setting is a sum of the closed side setting and the throw. This is calculated based on the closed side setting and the throw.

CO – There are three calculation options.

CO=0 - Parameterization

CO=1 - CANMET

CO=2 – Empirical

The model used for the process design is empirical. The Crushing Power Draw estimation is based on the following equation (from SME-Mineral Processing Handbook, Volume 1, S.W. Mudd Series, Page 3B-40)

$$\text{HP/ short ton} = (\text{WI} * ((\text{F}_{80})^{0.5} - (\text{P}_{80})^{0.5}) * \text{F}) / ((\text{F}_{80})^{0.5} * (\text{P}_{80})^{0.5})$$

Where,

WI = Work Index

$\text{F}_{80}$  = feed 80% passing size in microns

$\text{P}_{80}$  = product 80% passing size in microns

F = crushing factor, based on experience, which is 0.75 for primary crushing and 1.0 for secondary crushing

The jaw crusher and the roll crusher are also based on the same principle. However, for roll crusher, the length of the rolls, the roll diameter is to be specified. The throw for the cone and jaw crusher is set to industrial maximum of 7 inches.

**D.1.2. Mill Ball – MLB.** It can simulate single or multiple parallel ball mills.

There are three distinct calculation modes, which can be used in the ball mill:

Mode 1 – Simulation using Bond's Formula

Mode 2 – Parameterization

Mode 3 – Herbs Kinetic Model

The present model used the Mode 1 which uses Bond's formula as described.

Mode 1 – Simulation using Bond's Formula: The following options apply:

CO=1 Bond Inside Length. The mill inside length is input and the model calculates predicted product P80

CO=2 Bond Product P80. The mill circuit product P80 is input and the model estimates the optimum mill length.

CO=3 Bond Discharge D80. The mill discharge product D80 is input and the model estimates the optimum mill length.

Calculation options 1, 2, and 3 are based only on Bonds method. Calculation option 2 uses Bonds original method while 1 and 3 are modifications of this.

The mill is calculated in two stages.

1 - Bond's equations are used to determine the mill size and particle 80% passing size.

2 - Selection and breakage functions are used to calculate the complete product particle size analysis.

This two-stage calculation method was developed in 1981 and is reasonably accurate where only a Bond Work Index is known. If plant data is available, the open circuit design factor (OF) and the selection and breakage function coefficients can be adjusted to match actual plant data. (A discussion of the Bond formulas can be found in Chapter 23 of "Design and Installation of Comminution Circuits" published by the AIME).

Bond's equations are presented below. The normal ranges of values for grinding coefficients are:

$$BE = 0.50 \text{ to } 2.00 \quad (1.0) \text{ (recommended)}$$

$$AA[1] = 0.40 \text{ to } 2.00 \quad (1.1)$$

$$AA[3] = 1000 \text{ to } 4000 \quad (1600)$$

$$AA[2] = 0.70 \text{ to } 1.10 \quad (0.9)$$

$$AA[4] = 1.00 \text{ to } 4.00 \quad (3.00)$$

These values are incorporated in the design model for process design and power draw calculations.

The efficiency factors for grinding operation are as described below.

$$E1 = 1 \text{ for wet grinding}$$

$$E1 = 1.3 \text{ for dry grinding}$$

$$E2 = OF = 1.2 \text{ for 80 percent passing reference size}$$

## BIBLIOGRAPHY

1. J. P. Bennett, K.S. Kwong, "Refractory recycling-Concept to reality," *Environmental Issues and Waste Management Technologies VII, Ceramic Transactions*, Vol. 132, pp 3-15, 2002.
2. J. D. Smith, K. D. Peaslee, A. S. Barnes and H. Fang, "An economic, logistic, and technological approach to refractory recycling," *Proceedings of UNITECR'97*, pp-17-25, 1997.
3. J. P. Bennett, K. S. Kwong, "Spent refractory recycling/resuse efforts in the steel and aluminum industries," *Fourth International symposium, Recycling of metals and engineered materials, TMS*, pp 1353-1367, 2000.
4. R. T. Oxnard, "History and trends in refractory recycling: an integral part of waste minimization," *52<sup>nd</sup> Electric Furnace Conference, proceedings*, pp 397-400, 1994.
5. M. D. Crites, "Chrome-free refractories for copper production," *thesis-UMR*, pp 12-26, 1999.
6. M. D. Crites, M. Karakus, M. E. Schlesinger, M. Somerville and S. Sun, "Interaction of chrome-free refractories with copper smelting and converting slags," *Canadian Metallurgical Quarterly*, Vol. 39, pp 129-134, 2000.
7. K. S. Kwong and J. P. Bennett, "Recycling practices of spent MgO-C refractories," *Journal of Minerals & Materials Characterization & Engineering*, Vol. 1, pp 69-78, 2002.
8. A. G. M. Othman, W. M. N. Nour, "Recycling of spent magnesite and ZAS bricks for the production of new basic refractories," *Ceramics International*, Vol. 31, 1053-1059, 2005.
9. C. A. R. Gonzalez, W. F. Caley, and R. A. L. Drew, "Copper matte penetration resistance of basic refractories," *Metallurgical and Materials Transactions B*, Vol. 38B, pp 167-174, 2007.
10. K. S. Kwong, J. P. Bennett, and K. W. Collins, "The recycling of a 70%  $Al_2O_3$  spent refractory," *proceedings of UNITECR, refractories*, pp 487-496, 1997.
11. K. S. Kwong, J. P. Bennett, A. E. Wayne, III, "The recycling of spent refractories from a secondary brass producer," *Ceramics Transactions*, Vol. 87, pp 135-146, 1998.



12. Society for Mining, Metallurgy and Exploration, Inc. (SME), "Copper leaching, solvent extraction, and electrowinning technology," Ed. Gerald V. Jergensen pp 89-93, 1999.
13. J. Hur, S.Yim, and M. Schlautman, "Copper leaching from brake wear debris in standard extraction solutions", *Journal of Environ. Monit.*, Vol. 5, pp 837-843, 2003.
14. Mecucci and K.Scott, "Leaching and electrochemical recovery of copper, lead and tin from scrap printed circuit boards," *J. Chem. Technol Biotechnol*, Vol 77, pp 449-457, 2002.
15. F.R. Valenzuela, J.P.Andrade, J.Sapag, C.Tapia and C.Basualto, "The solvent extraction separation of molybdenum and copper from acid leach residual solution of Chilean molybdenite concentrate," *Minerals Engineering*, Vol.8, pp 893-900, 1995.
16. L.J. Bear and J. F.Moresby, "Recovery of copper from refractory furnace-lining bricks by segregation roasting," *Proc. Australas Inst. Min. Metall.*, No. 266, pp 21-27, 1976.
17. W. Hui, G. G.Hua, Q. Y. Feng, "Crushing performance and resource characteristic of printed circuit board scrap," *J. Cent. South Univ. Technol.*, Vol.12, pp 552-555, 2005.
18. G. C. Lowrison, "Crushing and Grinding: The Size reduction of solid materials," CRC Press, Inc., pp 17-30, 1994.
19. M.G. Nicholas, T.M. Valentine, M.J. Waite, "The wetting of alumina by copper alloyed with titanium and other elements," *Journal of Materials Science*, Vol. 15, pp 2197-2206, 1980.
20. C.C. Lin, R. B. Chen, R. K. Shiue, "A wettability study of Cu/Sn/Ti active braze alloys on alumina," *Journal of Materials Science*, Vol. 36, pp 2145-2150, 2001.
21. Meier, V.Gabriel, PR. Chidambaram, and G.R. Edwards, "Wetting and spreading of manganese and copper-manganese alloys on alumina surfaces," *Processing and Fabrication of Advanced Materials III*, Ed. V.A. Ravi, T.S. Srinivasan and J.J. Moore, The Minerals, Metals & Materials Society, pp 47-58, 1994.
22. P. D. Hoed, "An anatomy of furnace refractory erosion: Evidence from a pilot-scale facility," 58<sup>th</sup> Electric Furnace Conference Proceedings, Iron and Steel Society, pp 361-368, 2000.
23. M. Dekker, Inc., "Refractories Handbook," Ed. Charles A. Schacht, pp259-334, 2004.

24. C.C.Furnas, "Grading Aggregates, I-Mathematical relations for beds of broken solids of maximum density," *Industrial and Engineering chemistry*, Vol. 23, pp 1052-1058, 1981.
25. H.J.H. Brouwers, "Particle size distribution and packing fraction of geometric random packings," *Physical Review E*, Vol. 74, pp 0313091-0313091-14, 2006.
26. M. Glavind, E.J. Pedersen, "Packing calculations applied for concept mix design," *Proc. Creating with concrete*, University of Dundee, 1999.
27. J. E. Funk and D. R. Dinger, "Predictive process control of crowded particulate suspensions," pp 19-84, 1994.
28. F.C Bond, "Crushing & Grinding Calculations Part I," *British Chemical Engineering*, Vol. 6, pp. 378-385, 1961.
29. F.C Bond, "Crushing & Grinding Calculations Part II," *British Chemical Engineering*, Vol. 6, pp. 543-548, 1961.
30. Society of Mining Engineers, *SME Mineral Processing Handbook*, Ed. N.L. Weiss. New York: American Institute of Mining, Metallurgical, and Petroleum Engineers, Inc., pp. 30-71, 1985.
31. J.B. Mosher and C.B. Tague, "Conduct and precision of Bond Grindability Testing," *Minerals Engineering*, Vol. 14, pp 1187-1197, 2001.
32. B.A.Wills, "An introduction to the practical aspects of ore treatment and mineral recovery," *Mineral Processing Technology* 4<sup>th</sup> Edition, pp 200-253, 1980.
33. C.A.Rowland, "Selection of Rod Mills, Ball Mills and Re grind Mills," *Mineral Processing Plant Design, Practice, and Control Proceedings, Volume 1*, Eds. A.L. Mular, D.N. Halbe, and D.J. Barratt. Littleton, Colorado: Society for Mining, Metallurgy, and Exploration, Inc., pp. 710-754, 2002.
34. M.R. Ismael, R. Salomao and V.C. Pandolfelli, "Colloidal silica bonded refractory castables: optimization of the particle size distribution," *Refractories Applications and News*, Vol. 13, pp 10-15, 2008.

## VITA

Phani Krishna Angara Raghavendra was born on January 2, 1983. He received his primary and secondary education in India. In May of 2004, he received his bachelor's degree in Metallurgy and Materials Technology from Jawaharlal Nehru Technological University in India. After earning his undergraduate degree, he worked as a Junior Research Fellow at International Advanced Research Center in India for two years.

In December 2008, he received a master's degree in Materials Science Engineering from Missouri University of Science and Technology.